Vibration Suppression in a Traversing Mass - Cantilever Beam System

by

Yue Huang

A thesis

presented to Lakehead University

in fulfilment of the

thesis requirement for the degree of

Master of Science in Engineering

in

Control Engineering

Thunder Bay, Ontario, Canada, 2003

Your file Votre référence
ISBN: 0-612-92245-6
Our file Notre référence
ISBN: 0-612-92245-6

I hereby declare that I am the sole author of this thesis.

I authorize Lakehead University to lend this thesis to other institutions or individuals for the purpose of scholarly research.

I further authorize Lakehead University to reproduce this thesis by photocopying or by other means, in total or in part, at the request of other institutions or individuals for the purpose of scholarly research.

Lakehead University requires the signatures of all persons using or photocopying this thesis. Please sign below, and give address and date.

Abstract

A cantilever beam carrying a traversing spring-mass system is modeled. Applications of the system include robot traversing on space trusses, loads moving along stacker cranes carrying moving loads in large warehouse, and other such systems. The equations of motion are derived using Hamilton's principle. The obtained nonlinear partial differential equations are reduced to the nonlinear ordinary differential equations using Galerkin method. A novel method to control the vibration caused by the coupling between the beam and the moving subsystem is developed, which involves tuning the system to achieve internal resonance and then adding damping to the mass through a simple PD controller. Internal resonance's condition for the system is discussed through parametric analysis. Spectral analysis is carried out using FFT and a time-frequency analysis method.

Contents

List of Figures

List of Tables

Chapter 1

Introduction

1.1 Overview

The focus of this thesis is on the modeling and vibration suppression of a continuously distributed system interacting with a traversing spring-mass subsystem. The system has many applications from design of bridges, vibration suppression in stacker cranes carrying moving loads in large warehouse to vibration suppression in space trusses. The approach adopted can be summarized in the following aspects. Equations of motion are derived using Hamilton's principle and the resulting nonlinear partial differential equations of motion are reduced to nonlinear ordinary differential equations using Galerkin method. A vibration suppression strategy based on internal resonance is developed to suppress vibration in a traversing mass-cantilever beam system.

Hamilton's principle is commonly used to derive equations of motion for continuous system. The principle states that, of all the paths of admissible configurations

that the body can take as it goes from configuration 1 at time t_1 to configuration 2 at time t_2, the path that satisfies Newton's law at each instant during the interval is the path that extremizes the time integral of the difference between kinetic and potential energy of the system during the interval [1].

The equations of motion of the traversing mass-cantilever beam system obtained using Hamilton's principle are nonlinear partial differential equations. To solve these nonlinear partial differential equations, the equations first need to be discretized in the space and time domains and thus reduced to ordinary differential equations. Galerkin method is used for discretization.

Vibration suppression strategy is based on enhancing the coupling in the system. The coupling in the system can be made stronger by establishing internal resonance. When internal resonance exists in the system, energy imparted initially to one of the modes involved in the internal resonance will be continuously exchanged among all the modes involved in that internal resonance. When all the modes in the system are strongly coupled, damping applied in one direction can directly suppress vibrations in that direction and indirectly suppress vibrations in the remaining directions. internal resonance occurs if a commensurable or nearly commensuable relationship exists between the linear natural frequencies of the system. The novel feature of the vibration suppression technique presented in this thesis is establishing Internal Resonance between the beam and the traversing spring-mass subsystem as a prerequisite condition before suppressing vibrations with a simple PD controller. In order to establish internal resonance, parametric analysis is carried out to identify regions where the natural frequencies are commensurable or

nearly commensurable. Then, using a P controller-proportional gain controller, Internal Resonance is achieved. Having built up internal resonance and thus enhanced the coupling, damping is introduced in the traversing spring-mass subsystem via a D controller-derivative controller, resulting in rapid vibration suppression.

The vibration suppression technique developed is demonstrated using numerical simulation with the adaptive stepsize Runge-Kutta method and spectral analysis is carried out. Spectral analysis involves finding the response frequencies in the system using the well known discrete fourier transform. This approach gives the averaged behavior of the frequencies over the length of the time series for which the discrete fourier transform was performed. However, as will be shown in this work, the motion of the traversing spring-mass subsystem results in change in the response frequencies with time. To investigate this effect, time-frequency analysis is carried out. Time-frequency analysis captures the changes in the frequency content of a signal with time.

1.2 System Model

The system considered is shown in Figure 1.1. It consists of a flexible cantilever beam carrying a traversing spring-mass subsystem. The traversing spring-mass subsystem is a cart carrying a mass with two springs attached. One spring is in the horizontal plane and the other is in the vertical plane. The springs model the stiffnesses of the traversing spring-mass subsystem, and are not necessarily physical springs but can be actuators that provide position feedback to modify the stiffness characteristics of the traversing mass subsystem, so that the natural frequencies of

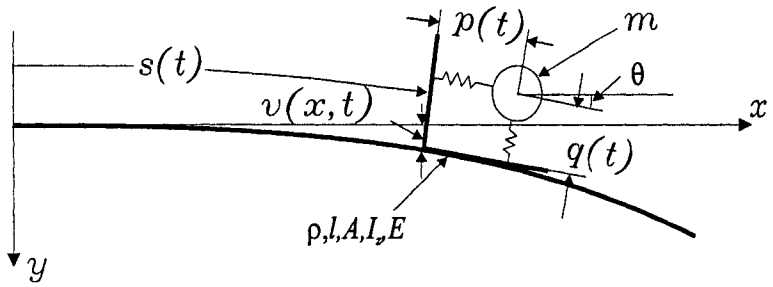

Figure 1.1: Beam and spring-mass system.

the system can be changed accordingly. The cart with the spring-mass is assumed to be in continuous contact with the beam at all times.

The beam is modeled as Euler-Bernoulli beam. Euler-Bernoulli beam is based on the assumption that plane cross sections of the beam remain plane and perpendicular to the neutral axis. The beam is assumed to be axially inextensible and shear force and rotatory inertia are not considered. Also small amplitude oscillations are assumed, thus geometric nonlinearities are not involved. The velocity and acceleration coupling between the beam and the moving spring-mass results in kinematic nonlinearities. Kinematic nonlinearities refer to the nonlinearities that arise due to coupling between different bodies, such as due to Coriolis and centripetal accelerations.

The equations of motion of the complete system are derived using Hamilton's principle. The equations are, in general, nonlinear-integral-partial-differential with some complex boundary conditions. These equations are difficult to solve analytically, therefore a numerical solution is pursued in this work.

1.3 Literature Survey

Elastic structures excited by moving loads have been investigated for more than a century. Historically the work originates in the earlier part of the nineteenth century with the design of railway bridges and later in other transportation engineering structures. Besides the above applications, similar problem arises in space structures ([2]) and systems such as cranes carrying moving loads ([3]).

The earliest relevant published paper is by Stokes [4] in 1849 where the motivation was the design of railway bridges. Later, Timoshenko [5] and Inglis [6] made further investigations about elastic structures excited by moving loads problem. A more recent book by Fryba [7] included analysis of beams with moving loads under different loading conditions. These early studies considered the moving mass as a moving force by neglecting the inertial forces caused by interaction between the structure and moving mass. Stanisic [8] presented a solution for the problem of a simply supported beam on an elastic foundation subject to a moving mass. Sadiku and Leipholz [9] studied the problem of an elastic beam under the actions of moving concentrated masses for typical end conditions, such as simply supported beam, cantilever beam, free-free end beam. Ting et al. [10] included an inertia term related to the local derivative of moving mass velocity in their analyses.

Due to the nature of the interaction between the moving mass and beam, many difficulties arise in obtaining solutions to the differential equations modeling the systems. To resolve these difficulties, many different methods have been proposed. Michaltsos et al. [11] derived a closed-form solution for a single-span beam carrying a moving mass by approximating the total time derivative of the mass displacement

with partial derivative and by using as a first approximation, the solution of the corresponding problem without the effect of the mass.

The finite-element method was applied to the moving force problem by Yoshida and Weaver [12], and later to the moving mass problem by Simkins [13], Olsson [14], Tanabe et al. [15] and Vu-Quoc , and Olsson [16, 17]. Cifuentes [18] introduced a combined finite element/finite-difference technique based on a Lagrange multiplier formulation that allows one to express the compatibility condition at the beam/mass interface.

A method based on expansion of the eigenfunctions in series has been utilized by Hutton and Counts [19], Stanisic [8], Akin and Mofid [20] and Olsson [21].

Ting et al. [10] and Sadiku and Leipholz [9] formulated the equation of motion for the system in the form of an integro-differential equation utilizing influence functions, which mathematically are Green functions. The work in [10] used the finite-difference method, and the work in [9] used the eigenfunctions expansion method.

Foda and Abduljabbar [22] studied the influence of the parameters of the system on the dynamic response of the beam subjected to a moving mass using the method of dynamic Green function.

Lee [23, 24] investigated the possibility of mass separation from the beam during the mass motion using the Lagrangian approach and the assumed mode method for Euler and Timoshenko beams.

In more recent times, much attention has been placed on modeling the dynamics and control of flexible structures. Many of these studies are motivated by the

International Space Station project. As an application of the beam carrying a moving mass problem, the project utilizes a Mobile Servicing System (MSS) which is used for transporting equipment, construction and maintenance of the space station. The MSS moves along a long slender flexible structure, and any manueuvering of the manipulator could induce undesirable vibration in the structure.

There have been many publications which deal with applications of control theory based method for vibration suppression in elastic structures without moving objects [25, 26]. Efforts have also been made to apply these methods to the case of flexible structures with a moving concentrated force [27, 28], which is a time-independent system.

Abdel-Rohman and Leipholz [29] presented the active control of a simply supported beam under a moving mass by using tensile and compressive bending moment generated using a single actuator.

Using the finite element approach with static control schemes, Frischgesell et al. [30] introduced a PID controller and a second controller that uses observer techniques to minimize the follower deflection of a continuous finite beam under a moving mass.

Lo [31] applied independent modal space control (IMSC) to reduce actively the vibration of the beam carrying a two-foot moving mass system. The approach in [31] was based on the idea of similarity transformations so that the dynamic system could be transferred into a block-diagonal Jordon form in terms of modal coordinates. Thus, a closed-loop controller could be designed for each second-order system independently in the modal space, one space regardless of the size of the

dynamic model. IMSC needs the same number of actuators as that of controller modes, resulting in a higher hardware cost.

Devasia et al. [32] used piezoactuator to reduce the deflection of flexible structures and presented techniques to determine the length and placement of piezoactuators for optimization of damping effect by collocated damping control, with linear quadratic cost functional as the initial condition and with the assumption of detectability and stabilizability, and minimum eigenvalue of controllability Grammian. Sung [33] designed a controller with full state feedback based on linearized equation of motion to reduce the deflection of the beam under a moving mass. In [33], two piezoelectric actuators were bonded along the bottom of the beam at different locations determined by the minimization of an optimal cost function. The non-linear effect was not accounted for in the design of the controller.

Compared to active controllers, passive controllers have permanent service time, and are easy to maintain and do not require external power supply. A passive control device, a tuned damper, was introduced by Kwon et al. [34] to control the vibration of a bridge under moving loads, where only vertical degrees of freedom of the moving loads were considered.

The motivation for the present work comes from Golnaraghi [35, 36] where the use of the moving mass as a controller to suppress vibration of the beam was proposed. The system analyzed in [35, 36] consists of a sliding mass-spring-dashpot mechanism attached to the end of a beam, resulting in a system with quadratic non-linearities. The spring was tuned to attain the 2:1 internal resonance. The damping coefficient was adjusted to obtain the optimal response. Duquette et al.

[37] demonstrated the effectiveness of utilizing 2:1 internal resonance to attenuate the vibration of a cantalever beam. The nonlinearity of the system in [37] was more dominant than that of [35, 36]. Experiment results were presented in [38]. Siddiqui et al.[39, 40, 41] investigated the dynamics of a beam carrying moving mass system under internal resonance conditions. These authors considered a spring-mass moving on a cantilever beam system. The moving mass had one degree of freedom and vibrates about the equilibrium position on the cantilever beam. To expand the application, in the present work, a more complex model is used with the spring-mass subsystem assumed to traverse the length of the beam rather than oscillating about a fixed equilibrium position. In addition, the mass is assumed to have two degrees of freedom.

1.4 Background Material

In this section, some background material is provided of the different methods available for investigating the dynamics of the system and some background material is provided.

1.4.1 Semi-discretization Methods

Dynamics of continuous systems are described using partial differential equations (PDEs). Before the PDEs can be solved, they need to be reduced to ordinary differential equations (ODEs). The reduction of PDEs in space and time to ODEs in time alone is referred as semi-discretization process. Separation of variables is one of the methods that can be used for the semi-discretization. In this method,

the solution is assumed to be in the form $w(x,t) = W(x)G(t)$, where $W(x)$ and $G(t)$ are obtained as solutions of corresponding semi-discretized equations. This method is often used in analysis of linear systems.

Rayleigh-Ritz method is another method that can be used for semi-discretization. Details of this method can be found in references, such as [1] and [42]. Rayleigh-Ritz method applied to solve equilibrium problems is described below:
Considering the following partial differential equation:

$$Lu(x,t) = f(x,t) \quad \text{in } V \tag{1.1}$$

where L is the partial differential operator. Equation (1.1) is subjected to the essential boundary conditions:

$$B_j u(x,t) = g_j(x,t) \quad j = 1,2,...,p \text{ on } S \tag{1.2}$$

where B_j is another partial differential operator. In (1.1) and (1.2), the independent variables x and t represent spatial coordinate and time, respectively. The dependent field variable $u(x,t)$ is to be determined by solving (1.1) and (1.2). In (1.1) and (1.2), f and g_j are known functions of the independent variables x and t. The integer p represents the number of boundary conditions, V is the field domain and S the boundary of the domain.

Equations (1.1) and (1.2) correspond to the functional I, given by:

$$I = \int_V F(x, u, u_x, u_{xx})dx \tag{1.3}$$

where $u_x = \frac{\partial u}{\partial x}$, $u_{xx} = \frac{\partial^2 u}{\partial x^2}$.

The displacement field u is approximated as:

$$\tilde{u} = \sum_{i=1}^{n} a_i(t)\phi_i(x) \tag{1.4}$$

where the functions $\phi_i(x)$ are known independent functions defined over V and S, and $\phi_i(x)$ satisfying the continuity requirements of (1.1) and the essential boundary conditions (1.2). The coefficient functions $a_i(t)$ are to be determined. The method involves determining the values of the coefficient functions $a_i(t)$ so as to extremize the functional I. After substituting (1.4) into (1.3), it becomes a function of the unknowns $a_i(t)$.

The necessary conditions for extremizing the functional I are given by:

$$\frac{\partial I(\tilde{u})}{\partial a_i} = 0 \tag{1.5}$$

which yields n ordinary differential equations for the unknown coefficient functions $a_i(t)$. The solution of these equations gives the approximated solution. It can be shown [43] that if $n \rightarrow \infty$ in this process, then u_n converges to the exact solution for the problem. When n is small, this method can give very good approximations to the exact solution if a judicious selection of the functions $\phi_0, \phi_1, \cdots, \phi_n$ is made.

In Rayleigh-Ritz method, a functional like I first needs to be found before discretization can be done. On the other hand, the Galerkin method which is used in this work employs partial differential equations as the starting point.

The method of weighted residuals is a general technique which can be regarded

as the basis for the Galerkin method [1]. A brief introduction of the method of weighted residuals and Galerkin method is presented below.

To illustrate the method, the partial differential equation (1.1) and the boundary conditions (1.2) are used. The displacement field u is approximated using (1.4). In general, $\tilde{u}$ will not satisfy the differential equation (1.1), thus a nonzero residual R would result, which is given by:

$$R(x, a_i) = L\tilde{u} - f \tag{1.6}$$

The method of weighted residuals requires finding the undetermined coefficient functions $a_i(t)$ that will make the residual R zero in a weighted average sense by requiring:

$$\langle w_j, R \rangle = \int_V w_j(x) R(x, a_i) dV = 0 \quad j = 1 \ldots N \tag{1.7}$$

where w_j are weighing functions and notation $\langle w_j, R \rangle$ denotes the weighed inner product. In the standard Galerkin method, the weighting functions $w_j(x)$ are chosen to be same as the basis functions $\phi_i(x)$. Equation (1.7) represents a system of N nonlinear ordinary differential equations which can be solved for $a_i(t)$.

1.4.2 Adaptive Stepsize Runge-Kutta Method

Using automatic ODEs solvers, such as the Runge-Kutta method, to solve ODEs obtained from PDEs using the semi-discretization approach is a challenging task. Gear [44] reports an overview of the automatic ODE solvers which can solve such equations. Adaptive stepsize Runge-Kutta method [45] is used in this work to solve

ODEs. The purpose of adaptive stepsize control is to achieve some predetermined accuracy in the solution with minimum computation effort. Runge-Kutta method is a common numerical technique for solving initial value problems. It propagates a solution over each step by combining results from several Euler-style steps (each involving one evaluation of the functions of f, where f are defined as $\frac{dy_i(x)}{dx} = f_i(x, y_1, ..., y_n), i = 1, ..., N$), and then using the information obtained to match a Taylor series expansion up to some higher order. The step size is adjusted according to an estimate of the truncation error. The step size adjustment algorithm used here is based on the Runge-Kutta-Fehlberg formulas.

1.4.3 Time-Frequency Analysis Method

After the equations of motion are semi-discretized and then solved using adaptive stepsize Runge-Kutta method, the time response of the system can be obtained. When the cart with the spring-mass moves along the beam, the natural frequencies of the system change with the position of the cart. To capture the change in the frequencies with time, time-frequency analysis is required. The power spectrum, which is obtained by taking the discrete fourier transform (DFT) of the time series and computing the power (mean squared amplitude) at the various frequencies, gives the averaged behavior over the length of time series. On the other hand, in time varying system, the local spectral behavior is of more interest. The local spectral behavior is studied using a spectrograph. The spectrograph is obtained by finding the power spectrum of relatively small segments of data and the results are displayed on time and frequency axes, with time corresponding to the center of

the data segment. The power is shown using a grey scaling for the whole plot. For smoother transitions, the data segments are overlapped.

1.5 Thesis Outline

In this thesis, Chapter 2 deals with modeling and semi-discretization. The equations of motion are derived using Hamilton's principle. The obtained integral partial differential equations are reduced to a symmetric form first and then reduced to nonlinear ordinary differential equations using Galerkin method.

Chapter 3 presents the vibration suppression methodology using internal resonance. Parametric analysis is also carried out and the results are presented.

In Chapter 4, the effectiveness of the vibration suppression strategy is demonstrated through numerical simulation. Dynamics of the system is studied in detail using time-frequency analysis.

In Chapter 5 the conclusions for this thesis are drawn.

Chapter 2

Modeling

In this chapter, a cantilever beam carrying a traversing spring-mass subsystem model shown in Figure 2.1 is modeled. Equations of motion are derived using an energy approach. The equations of motion obtained are nonlinear partial differential equations, which are discretized using Galerkin method resulting in semi-discretized nonlinear ordinary differential equations.

2.1 System Parameters

The various parameters used in the system modeling have already been shown in Figure 2.1. Figure 2.1 is the same as Figure 1.1. It is repeated here for completeness. The beam parameters are length (l), area of cross-section (A), volume density (ρ), area moment of inertia about the z axis (I_z), and the modulus of elasticity (E). The traversing spring-mass parameters include the moving mass (m), spring stiffness of the moving mass parallel to the length of the beam (k_p), spring stiffness

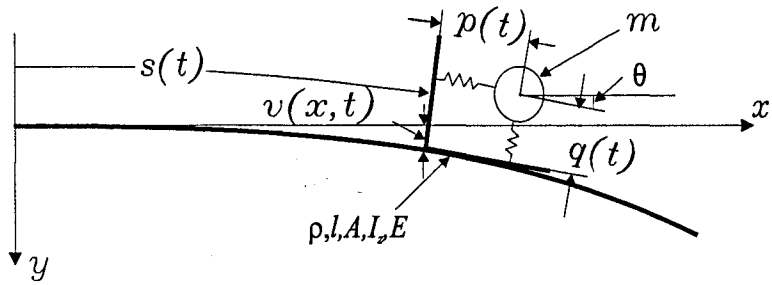

Figure 2.1: Beam and spring-mass system.

of the moving mass perpendicular to the length of the beam (k_q). The position of the spring-mass subsystem is measured by a curvilinear coordinate $s(t)$. The displacement of the reference axis is measured by $v(x,t)$ as shown in Figure 2.1. The displacement of the moving mass about its equilibrium position p_e and q_e are measured by $p(t)$ parallel to the length of the beam, and $q(t)$ perpendicular to the length of the beam.

2.1.1 Nondimensional Parameters

Nondimensional parameters are used in this work. The nondimensionalized parameters are defined as below:

$$\begin{array}{llll} \hat{s} = \frac{s}{l} & \hat{p} = \frac{p}{l} & \hat{q} = \frac{q}{l} & \hat{x} = \frac{x}{l} \\ \hat{y} = \frac{y}{l} & \hat{v} = \frac{v}{l} & \hat{A} = \frac{A}{l^2} & \hat{m} = \frac{m}{\rho A l} \\ \hat{I}_z = \frac{I_z}{Al^2} & \hat{t} = \frac{t}{\sqrt{\frac{\rho A l^4}{EI_z}}} & \omega_p^2 = \frac{k_p \rho A l^4}{mEI_z} & \omega_q^2 = \frac{k_q \rho A l^4}{mEI_z} \end{array} \tag{2.1}$$

For convenience, the (ˆ)s are dropped. In the work that follows only nondimensionalized parameters are used.

2.2 Lagrangian

Hamilton's principle is used to develop the equations of motion. To use Hamilton's principle, Lagrangian of the system needs to be obtained first. Lagrangian $\mathcal{L}$ is the difference between the kinetic energy T and the potential energy V of the system. The kinetic energy, the potential energy and Lagrangian $\mathcal{L}$ are derived in Sections 2.2.1-2.2.7.

2.2.1 Displacement Field

Displacements based on Euler-Bernoulli beam model are shown in Figure 2.2.

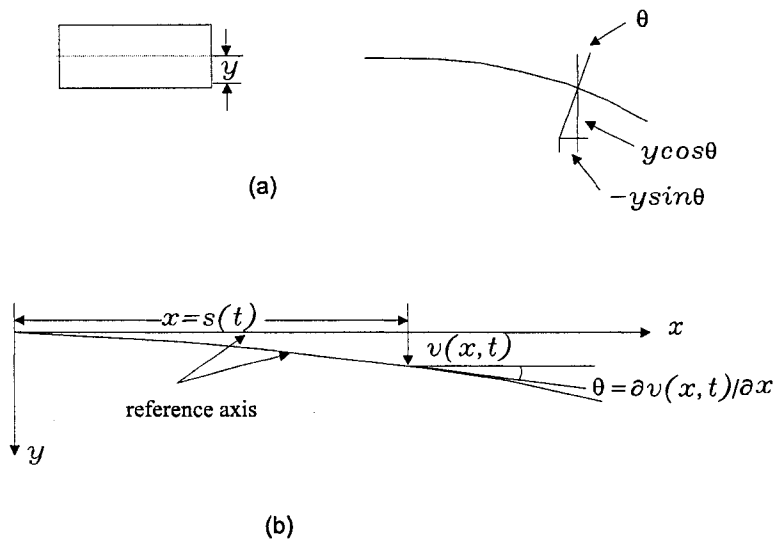

Figure 2.2: Deformation. (a) Displacement of a point located at a distance y below the reference axis, (b) Deflection of the reference axis.

The following displacement field describes the displacement of a point located at a

distance y below the reference axis.

$$\begin{aligned} u_x &= -y\sin(\theta), \quad \sin(\theta) = \left(\frac{\partial}{\partial x}v(x,t)\right) \\ u_y &= v(x,t), \quad \cos(\theta) = 1 \\ u_z &= 0 \end{aligned} \tag{2.2}$$

where u_x, u_y and u_z are the displacements along x, y and z directions respectively. Because small vibrations are assumed for the beam, θ is small. Therefore $\cos(\theta) = 1$.

2.2.2 Strains

Since the deformations are assumed to be small, linear strain displacement relationships are used to derive the strain distribution in the beam. Strain field is thus obtained using the following relationship [1]:

$$\epsilon_{ij} = \frac{1}{2}\left(\frac{\partial u_i}{\partial x_j} + \frac{\partial u_j}{\partial x_i}\right) \tag{2.3}$$

where the indices $i, j = 1, 2, 3$ corresponds to x, y and z coordinates, respectively. The subscripts in ϵ_{ij} represent the plane i and the direction j in which the strain ϵ_{ij} acts. Substituting (2.2) into (2.3) results in only one nonzero strain term, which is the strain acting on the x plane in the x direction, given by:

$$\begin{aligned} \epsilon_{xx} &= -y\frac{\partial \theta}{\partial x} \\ \frac{\partial \theta}{\partial x} &= \frac{\partial^2 v(x,t)}{\partial x^2} \end{aligned} \tag{2.4}$$

2.2.3 Strain Energy

The strain energy of the beam is given by :

$$U = \frac{1}{2}\int_{\mathcal{V}} \epsilon_{xx}^2 d\mathcal{V} \tag{2.5}$$

where $\mathcal{V}$ is the nondimensionalized volume of the beam. It follows that if the nondimensionalised parameters, (2.1) are used, all the energy terms in the Lagrangian will have a multiplying factor $\frac{EI_z}{l}$ (has units of work). This factor appears as a constant multiplying the equations of motion. This constant would factor out when the nondimensionalized variables are substituted in the equations of motion. Therefore it can be dropped out from all the energy terms. After substituting (2.4) into (2.5) and dropping out the factor term, the strain energy is obtained as :

$$U = \frac{1}{2}\int_0^1 \left(\frac{\partial\theta}{\partial x}\right)^2 dx \tag{2.6}$$

2.2.4 Kinetic Energy of the Beam

The velocity field is obtained by differentiating the displacement field (2.2) with time and is obtained as:

$$\begin{aligned} \dot{u}_x &= -y\cos(\theta)\frac{\partial\theta}{\partial t} \\ \dot{u}_y &= \frac{\partial v}{\partial t} \end{aligned} \tag{2.7}$$

Because the rotatory inertial term is small compared to the other terms, $\dot{u}_x$ is not included in kinetic energy. The kinetic energy of the beam is therefore,

$$T_b = \frac{1}{2}\int_0^1 \left(\frac{\partial v}{\partial t}\right)^2 dx \tag{2.8}$$

2.2.5 Kinetic Energy of the Mass

The velocity of the moving mass is obtained from Figure 1.1 as:

$$\begin{aligned} \dot{u}_{mx} &= [\dot{u}_x + \dot{s}\cos(\theta) + \dot{p}\cos(\theta) - \dot{q}\sin(\theta)]\Big|_{x=s(t)} \\ \dot{u}_{my} &= [\dot{u}_y + \dot{s}\sin(\theta) + \dot{p}\sin(\theta) + \dot{q}\cos(\theta)]\Big|_{x=s(t)} \end{aligned} \tag{2.9}$$

where $\dot{s}(t)$ is the cart's velocity along the length of the beam, $\dot{p}(t)$ is the velocity of the mass along the length of the beam measured relative to the cart, $\dot{q}(t)$ is the velocity of the mass perpendicular to the length of the beam measured relative to the cart, $\dot{u}_{mx}$ and $\dot{u}_{my}$ are the velocity components of the mass along x and y coordinates respectively. It should be noted that $\dot{u}_{mx}$ and $\dot{u}_{my}$ depend on the position of the traversing spring-mass subsystem. The kinetic energy of the moving mass can be expressed by the following equations:

$$\begin{aligned} T_m &= \frac{1}{2}m(\dot{u}_{mx}^2 + \dot{u}_{my}^2)\Big|_{x=s(t)} \\ &= \frac{1}{2}m[(-y\dot{\theta}\cos(\theta) + \dot{s}\cos(\theta) + \dot{p}\cos(\theta) - \dot{q}\sin(\theta))^2 \\ &\quad +(\dot{v} + \dot{s}\sin(\theta) + \dot{p}\sin(\theta) + \dot{q}\cos(\theta))^2]\Big|_{x=s(t)} \end{aligned} \tag{2.10}$$

After neglecting rotatory inertial terms, the kinetic energy of the moving mass is given by:

$$\begin{aligned} T_m &= m\left[\left(\dot{p}+\frac{\partial v}{\partial t}\sin(\theta)\right)\dot{s}+\frac{\partial v}{\partial t}\sin(\theta)\dot{p}\right. \\ &\quad \left.+\frac{\partial v}{\partial t}\dot{q}+\frac{1}{2}\left(\frac{\partial v}{\partial t}\right)^2\right]\Bigg|_{x=s(t)} \\ &\quad +\frac{1}{2}m\dot{s}^2+\frac{1}{2}m\dot{p}^2+\frac{1}{2}m\dot{q}^2 \end{aligned} \tag{2.11}$$

2.2.6 Potential Energy of the Springs

The potential energy of the springs attached to the mass is given by :

$$V_m = \frac{1}{2}m\omega_p^2(p-p_e)^2+\frac{1}{2}m\omega_q^2(q-q_e)^2 \tag{2.12}$$

where p_e and q_e are the equilibrium positions of the moving mass corresponding to the variables $p(t)$ and $q(t)$, and ω_p and ω_q are the corresponding nondimensional frequencies of the spring-mass subsystem.

2.2.7 Lagrangian

The Lagrangian can be obtained from the energy terms derived in Section 2.2.1-2.2.6 and is given by:

$$\begin{aligned} \mathcal{L} &= T-V \\ &= T_b(\dot{v})+T_m(s,\dot{s},\dot{p},\dot{q},\dot{v},v')-U(v'')-V_m(p,q) \end{aligned} \tag{2.13}$$

where T_b is the kinetic energy of the beam, T_m is the kinetic energy of the moving mass, U is the strain energy of the beam and V_m is the potential energy of the springs. $()'$ indicates differentiation with respect to x and $\dot{()}$ indicates differentiation with respect to time.

2.3 Hamilton's Principle

Hamilton's principle is applied to obtain the equations of motion of the system. This involves taking the first variation of the time integral of the Lagrangian:

$$\delta^{(1)} \int_{t_1}^{t_2} \mathcal{L} dt = 0 \tag{2.14}$$

where the Lagrangian is given by (2.13).

2.3.1 Equations of Motion

Taking variations of (2.13) in the usual way [1] gives the following form for the equations of motion :

p variation:

$$\left[\frac{\partial^2 T_m}{\partial t \partial \dot{p}} + \frac{\partial^2 T_m}{\partial x \partial \dot{p}} \frac{\partial s}{\partial t}\right]_{x=s(t)} + \frac{\partial V_m}{\partial p} = 0 \tag{2.15}$$

q variation:

$$\left[\frac{\partial^2 T_m}{\partial t \partial \dot{q}} + \frac{\partial^2 T_m}{\partial x \partial \dot{q}} \frac{\partial s}{\partial t}\right]_{x=s(t)} + \frac{\partial V_m}{\partial q} = 0 \tag{2.16}$$

v variation:

$$\left[\frac{\partial^2 T_m}{\partial t \partial \dot{v}} + \frac{\partial^2 T_m}{\partial x \partial \dot{v}} \frac{\partial s}{\partial t}\right]_{x=s(t)} + \int_0^1 \left\{ \frac{d}{dt}\left(\frac{\partial T_b}{\partial \dot{v}}\right) + \frac{d^2}{dx^2}\left(\frac{\partial U}{\partial v''}\right)\right\} dx = 0 \quad (2.17)$$

The accompanying boundary conditions are given by:

$$\left(\frac{\partial^2 U}{\partial x \partial v''}\right)_{x=1} = 0$$
$$\left(\frac{\partial U}{\partial v''}\right)_{x=1} = 0 \quad (2.18)$$

Substituting the energy terms (2.6), (2.8), (2.11) and (2.12) into (2.15), (2.16) and (2.17), the following equations are obtained:

p variation:

$$\left(\frac{\partial^2}{\partial t^2} p(t)\right) + \omega_p^2 (p(t) - p_e) + \left(\frac{\partial^2}{\partial t^2} s(t)\right) + \left[\left(\frac{\partial^2}{\partial t^2} v(x,t)\right)\left(\frac{\partial}{\partial x} v(x,t)\right) + \left(\frac{\partial}{\partial t} v(x,t)\right)\left(\frac{\partial^2}{\partial x \partial t} v(x,t)\right) + \left(\frac{\partial}{\partial t} s(t)\right)\left(\frac{\partial^2}{\partial x \partial t} v(x,t)\right)\left(\frac{\partial}{\partial x} v(x,t)\right) + \left(\frac{\partial}{\partial t} s(t)\right)\left(\frac{\partial}{\partial t} v(x,t)\right)\left(\frac{\partial^2}{\partial x^2} v(x,t)\right)\right]\Big|_{x=s(t)} = 0 \quad (2.19)$$

q variation:

$$\left(\frac{\partial^2}{\partial t^2} q(t)\right) + \omega_q^2 (q(t) - q_e) + \left[\left(\frac{\partial^2}{\partial t^2} v(x,t)\right)\right.$$

$$+\left(\frac{\partial}{\partial t}s(t)\right)\left(\frac{\partial^2}{\partial x \partial t}v(x,t)\right)\Bigg]\Bigg|_{x=s(t)} = 0 \qquad (2.20)$$

v variation:

$$\begin{aligned} m\Bigg[&\left(\frac{\partial^2}{\partial t^2}s(t)\right)\left(\frac{\partial}{\partial x}v(x,t)\right)+\left(\frac{\partial^2}{\partial t^2}p(t)\right)\left(\frac{\partial}{\partial x}v(x,t)\right)\\ &+\left(\frac{\partial^2}{\partial t^2}q(t)\right)+\left(\frac{\partial^2}{\partial t^2}v(x,t)\right)\\ &+2\left(\frac{\partial}{\partial t}s(t)\right)\left(\frac{\partial^2}{\partial x \partial t}v(x,t)\right)+\left(\frac{\partial}{\partial t}p(t)\right)\left(\frac{\partial^2}{\partial x \partial t}v(x,t)\right)\\ &+\left(\frac{\partial}{\partial t}s(t)\right)^2\left(\frac{\partial^2}{\partial x^2}v(x,t)\right)\\ &+\left(\frac{\partial}{\partial t}s(t)\right)\left(\frac{\partial}{\partial t}p(t)\right)\left(\frac{\partial^2}{\partial x^2}v(x,t)\right)\Bigg]_{x=s(t)}\\ &+\int_0^1\left[\left(\frac{\partial^2}{\partial t^2}v(x,t)\right)+\left(\frac{\partial^4}{\partial x^4}v(x,t)\right)\right]dx = 0 \end{aligned} \qquad (2.21)$$

In (2.21), the terms outside the integral are nonlinear coupling terms. The first two terms come from the acceleration of the mass in the x direction, the third term is from the acceleration of the mass in the y direction, the fourth term is the acceleration term of the beam in the y direction, the fifth term represent the Coriolis acceleration, the sixth term has the form of Coriolis acceleration and the remaining two terms represent the centripetal acceleration. All these acceleration terms arise due to the inertial nonlinear coupling between the mass and the beam and need to be evaluated at the position of the traversing spring-mass subsystem. In (2.19)-(2.21), partial derivative notation is used for functions with only one independent variable (for example, $p(t)$, $q(t)$ and $s(t)$) for convenience. Since this does not cause

any mathematical inconsistency, it will be used through out the work.

The natural boundary conditions corresponding to the equations of motion (2.19)-(2.21) are given by:

$$\begin{aligned} \left(\frac{\partial^3}{\partial x^3}v(x,t)\right)\Big|_{x=1} &= 0 \\ \left(\frac{\partial^2}{\partial x^2}v(x,t)\right)\Big|_{x=1} &= 0 \end{aligned} \tag{2.22}$$

The first and the second equation in (2.22) represent the shear force and moment force at the free end of the beam are zero respectively. At the fixed end, the corresponding boundary conditions are given by:

$$\begin{aligned} v(x,t)\,|_{x=0} &= 0 \\ \left(\frac{\partial}{\partial x}v(x,t)\right)\Big|_{x=0} &= 0 \end{aligned} \tag{2.23}$$

The first and the second equation in (2.23) represent the deflection and slope at the fix end of the beam are zero respectively.

2.4 Initial Values

It is assumed that there is no external force working on the beam carrying moving spring-mass system, thus only free vibrations are analyzed using the following

prescribed initial values:

$$\begin{aligned} p(0) &= p_0 & \left.\frac{\partial p(t)}{\partial t}\right|_{t=0} &= 0 \\ q(0) &= q_0 & \left.\frac{\partial q(t)}{\partial t}\right|_{t=0} &= 0 \\ v(x,0) &= v_0(x) & \left.\frac{\partial v(x,t)}{\partial t}\right|_{t=0} &= 0 \end{aligned} \tag{2.24}$$

where p_0 and q_0 represent the initial displacements of the mass, $v_0(x)$ represents the initial deflection curve of the beam and the initial velocities for $p(t)$, $q(t)$and $v(x,t)$ are assumed to be zero.

The initial values for the beam must satisfy the boundary conditions. Thus, the scaled first mode shape of a cantilever beam is used as the initial deflection curve of the beam, which is expressed as:

$$\begin{aligned} v_0(x) &= \frac{v_{t0}}{2}(\cosh(k_1 x) - \cos(k_1 x) \\ &- \frac{\cos(k_1)+\cosh(k_1)}{\sin(k_1)+\sinh(k_1)}(\sinh(k_1 x) - \sin(k_1 x))) \end{aligned} \tag{2.25}$$

where v_{t0} is the initial tip deflection of the beam and $k_1 = 1.8751$ is a constant corresponding to the first mode shape of a cantilever beam.

2.5 Spatial Discretization

The equations of motion (2.19)-(2.21) are partial differential equations. Galerkin method is used to reduce the partial differential equations to the ordinary differential equations. To apply Galerkin method, the equations of motion are multiplied by a weighting function. Then, integration by parts is carried out, resulting in

reduction in the continuity requirement for the solution due to the reduction in the degree of the highest derivative appearing in the equations. For example, the highest spatial derivative appearing in the beam equation is of fourth order, thus it requires that the solution for the beam's displacement must have continuous fourth derivative, but through integrating by parts, the requirement is reduced to the second order continuous derivative.

Eigenfunctions of a cantilever beam are used as basis functions in Galerkin method. The eigenfunctions of a cantilever beam satisfy the continuity requirements of the resulting differential equations as well as boundary conditions. It should be noted that the eigenfunctions of a cantilever beam do not account for the effect of the moving mass and are not the eigenfunctions of the complete system. They are also not the exact solutions of the equations of motion obtained in the method of separation of variables. But they are used here as basis functions in Galerkin method because they satisfy the continuity requirment of the problem. Another advantage of this process is that the natural boundary conditions are incorporated during the integration by parts.

2.5.1 Symmetric Formulation

A symmetric formulation renders the continuity requirments for the variables to be solved the same. To obtain a symmetric formulation, the equations of motion are multiplied by a weighing function $w(x)$ and then integrated by parts. The natural boundary conditions (2.22) are incorporated into the equations of motion during integration by parts. The equations for the mass motion (2.19) and (2.20) have

no space integration terms, so therefore spatial discretization is not required. The following equations are obtained after applying the procedure:

$$\left(\frac{\partial^2 p}{\partial t^2}\right) + \omega_p^2(p - p_e) + \left(\frac{\partial^2 s}{\partial t^2}\right) + \left[\left(\frac{\partial^2 v}{\partial t^2}\right)\left(\frac{\partial v}{\partial x}\right) + \left(\frac{\partial v}{\partial t}\right)\left(\frac{\partial^2 v}{\partial x \partial t}\right) + \left(\frac{\partial s}{\partial t}\right)\left(\frac{\partial^2 v}{\partial x \partial t}\right)\left(\frac{\partial v}{\partial x}\right) + \left(\frac{\partial s}{\partial t}\right)\left(\frac{\partial v}{\partial t}\right)\left(\frac{\partial^2 v}{\partial x^2}\right)\right]\Big|_{x=s(t)} = 0 \tag{2.26}$$

$$\left(\frac{\partial^2 q}{\partial t^2}\right) + \omega_q^2(q - q_e) + \left[\left(\frac{\partial^2 v}{\partial t^2}\right) + \left(\frac{\partial s}{\partial t}\right)\left(\frac{\partial^2 v}{\partial x \partial t}\right)\right]\Big|_{x=s(t)} = 0 \tag{2.27}$$

$$m\left[\left(\frac{\partial^2 s}{\partial t^2}\right)\left(\frac{\partial v}{\partial x}\right)w + \left(\frac{\partial^2 p}{\partial t^2}\right)\left(\frac{\partial v}{\partial x}\right)w + 2\left(\frac{\partial s}{\partial t}\right)\left(\frac{\partial^2 v}{\partial x \partial t}\right)w + \left(\frac{\partial p}{\partial t}\right)\left(\frac{\partial^2 v}{\partial x \partial t}\right)w + \left(\frac{\partial^2 q}{\partial t^2}\right)w + \left(\frac{\partial^2 v}{\partial t^2}\right)w + \left(\frac{\partial s}{\partial t}\right)^2\left(\frac{\partial^2 v}{\partial x^2}\right)w + \left(\frac{\partial s}{\partial t}\right)\left(\frac{\partial p}{\partial t}\right)\left(\frac{\partial^2 v}{\partial x^2}\right)w\right]_{x=s(t)} + \int_0^1 \left[\left(\frac{\partial^2 v}{\partial t^2}\right)w + \left(\frac{\partial^2 v}{\partial x^2}\right)\left(\frac{\partial^2 w}{\partial x^2}\right)\right]dx = 0 \tag{2.28}$$

where (2.26) and (2.27) are the repeat of (2.19) and (2.20). The formulation (2.26)-(2.28) is referred to as the symmetric formulation because $v(x,t)$ and $w(x)$ have the same highest order derivative.

2.5.2 Implementation of Spatial Discretization

The following expansions are used for the Galerkin method:

$$\begin{aligned} v(x,t) &= \sum_i \alpha_i(t)\phi_i(x) \\ w(x) &= \sum_i w_i\phi_i(x) \end{aligned} \tag{2.29}$$

where i varies from 1 to n, $\alpha_i(t)$ are coefficient functions, $\phi_i(x)$ are basis functions and w_i are weighing function coefficents. The symmetric formulation renders the continuity requirments for both $v(x,t)$ and $w(x)$ the same. Therefore the same basis functions ϕ_i are chosen for $v(x,t)$ and $w(x)$. The number of basis functions for both v and w are also assumed to be equal. The undetermined coefficients w_i are arbitrary. Now, substituting (2.29) into the equations of motion (2.26)- (2.28) and setting w_i to one when $i = j$ and to zero when $i \neq j$ give the i^{th} semi-discretized ordinary differential equation. The semi-discretized ordinary differential equations are thus obtained as:

p equation:

$$\begin{aligned} \ddot{p} + \ddot{s} + \omega_p^2(p - p_e) + \dot{s}\left[\phi_i\phi_j'' + \phi_i'\phi_j'\right]_{x=s(t)}\{\dot{\alpha}_i\alpha_j\} \\ + \left[\phi_i\phi_j'\right]_{x=s(t)}\{\dot{\alpha}_i\dot{\alpha}_j + \ddot{\alpha}_i\alpha_j\} &= 0 \end{aligned} \tag{2.30}$$

q equation:

$$\ddot{q} + \omega_q^2(q - q_e) + \dot{s}\left[\phi_i'\right]_{x=s(t)}\{\dot{\alpha}_i\} + \left[\phi_i\right]_{x=s(t)}\{\ddot{\alpha}_i\} = 0 \tag{2.31}$$

v equation:

$$\begin{aligned} & m\left\{\left[\phi_i\phi_j\right]_{x=s(t)}\left\{\ddot{\alpha}_j\right\}+\ddot{q}\left\{\phi_i\right\}_{x=s(t)}\right. \\ & +\left[\phi_i\phi_j'\right]_{x=s(t)}\left\{\left(\ddot{p}+\ddot{s}\right)\left\{\alpha_j\right\}+\left(2\dot{s}+\dot{p}\right)\left\{\dot{\alpha}_j\right\}\right\} \\ & \left.+\left(\dot{s}\dot{p}+\dot{s}^2\right)\left[\phi_i\phi_j''\right]_{x=s(t)}\left\{\alpha_j\right\}\right\} \\ & +\left[\int_0^1\phi_i\phi_j dx\right]\left\{\ddot{\alpha}_j\right\}+\left[\int_0^1\phi_i''\phi_j'' dx\right]\left\{\alpha_j\right\} = 0 \end{aligned} \tag{2.32}$$

where the repeated indices imply summation over the index, $\lfloor\cdots\rfloor$ denotes a row matrix , $\{\cdots\}$ denotes a column matrix and $[\cdots]$ denotes a square matrix. Equations (2.30), (2.31) and (2.32) are ordinary differential equations with kinematic nonlinearities. The kinematic nonlinearities come from the coupling between the moving mass and the beam. The number of equations of motion depend on the number of basis functions ϕ_i used for the approximation. These basis functions are given in the following sub-section.

2.5.3 Eigenfunctions of a Cantilever Beam

Eigenfunctions of a cantilever beam are chosen to be the basis functions for Galerkin method. They are simple and satisfy the continuity requirements and boundary conditions. The first four eigenfunctions of a cantilever beam are used as basis functions. The solution converges with using the first four eigenfunctions through trial and error. Increasing the numbers of basis functions increases the accuracy of the solution, but makes problem solving more costly.

The cantilever beam eigenfunctions in nondimensionalized parameters are given

by :

$$\phi_i = \cosh(k_i x) - \cos(k_i x) - \frac{\cos(k_1) + \cosh(k_i)}{\sin(k_i) + \sinh(k_i)}(\sinh(k_i x) - \sin(k_i x)) \tag{2.33}$$

For the first four modes, k_i have the values

$$k_1 = 1.875104069, k_2 = 4.694091133, k_3 = 7.854757438, k_4 = 10.995547073 \tag{2.34}$$

Mass and stiffness matrices and stiffness matrix can be calculated by integrating the products of basis functions and their second derivatives over the length of the beam, which are,

$$[M_{ij}] = \left[\int_0^1 \phi_i \phi_j dx\right] = \begin{bmatrix} 1 & 0 & 0 & 0 \\ 0 & 1 & 0 & 0 \\ 0 & 0 & 1 & 0 \\ 0 & 0 & 0 & 1 \end{bmatrix} \tag{2.35}$$

$$[K_{ij}] = \left[\int_0^1 \phi_i'' \phi_j'' dx\right] = \begin{bmatrix} 12.36236340 & 0 & 0 & 0 \\ 0 & 485.5188211 & 0 & 0 \\ 0 & 0 & 3806.546524 & 0 \\ 0 & 0 & 0 & 14617.25610 \end{bmatrix} \tag{2.36}$$

The other matrix terms in (2.30), (2.31) and (2.32) need to be evaluated at the

position of the moving cart. They are assembled online.

In this chapter, the system model was developed and the equations of motion were derived. The obtained partial differential equations of motion were semi-discretized using Galerkin method. In the next chapter, the internal resonance conditions will be investigated through parametric analysis.

Chapter 3

Vibration Suppression Strategy

The vibration suppression strategy used in this work is based on enhancing the coupling in an n-degree freedom system using Internal Resonance. An n-degree-freedom system has n linear natural frequencies and n corresponding modes of vibration. Denoting these frequencies by $f_1, f_2, \cdots, f_n$, whenever two or more of these frequencies are commensurable or nearly commensurable, internal resonance occurs [46]. Commensurability implies that frequencies are in an integral ratio, that is $n_1 f_1 + n_2 f_2 + ... + n_i f_i$, where $i = 1, ..., n$ and n_i are integral constants. Depending on the order of the nonlinearity in the system, the commensurable relationships of frequencies can result in the corresponding modes to be strongly coupled. For a two-degree-freedom system with linear coupling, internal resonance occurs if $f_1 \approx f_2$. Similarly, for a two degrees of freedom system with quadratic nonlinearities, internal resonance can occur if $f_1 \approx 2f_2$.

When a system undergoing free vibration is under internal resonance, energy imparted initially to one of the modes will be continuously exchanged among all

the modes involved in internal resonance. If damping is present in the system, then the energy will be continuously reduced as it is being exchanged. For the system under consideration, when internal resonance is established between the beam and the traversing spring-mass subsystem, the vibration of the beam can be diminished indirectly by adding damping to the moving mass while the vibration of the moving mass is also reduced due to the direct damping effect. To analyze internal resonance, Taylor series expansion is applied to linearize the equations of motion about the equilibrium points and natural frequencies of the system are obtained. To identify regions in the parameter space where the vibration suppression strategy can be applied, variation in natural frequencies of the linearized system is investigated through parametric analysis.

3.1 Linearized Equations of Motion

Equations of motion are linearized about the equilibrium positions. It can be seen from (2.30), (2.31) and (2.32) that the equilibrium position for p is p_e, that for q is q_e and those for α_i are zero (obtained by setting velocities and accelerations to zero). The first order Taylor series expansion of (2.30), (2.31) and (2.32) about the equilibrium positions $p = p_e, q = q_e$ and $\alpha_i = 0$ are shown below:

$$\begin{aligned} \ddot{p} + \omega_p^2 p &= 0 \\ \ddot{q} + \omega_q^2 q + \dot{s} \left\lfloor \phi_i' \right\rfloor_{x=s(t)} \{\dot{\alpha}_i\} + \left\lfloor \phi_i \right\rfloor_{x=s(t)} \{\ddot{\alpha}_i\} &= 0 \\ m \left\{ \ddot{q} \{\phi_i\}_{x=s(t)} + [\phi_i \phi_j]_{x=s(t)} \left\{ \{\ddot{\alpha}_j\} + \dot{s}^2 \left[\phi_i \phi_j''\right]_{x=s(t)} \{\alpha_j\} \right\} \right. & \end{aligned}$$

$$+\left[\phi_i\phi_j'\right]_{x=s(t)}\left\{\ddot{s}\left\{\alpha_j\right\}+2\dot{s}\left\{\dot{\alpha}_j\right\}\right\}$$
$$+\left[\int_0^1\phi_i\phi_j dx\right]\left\{\ddot{\alpha}_j\right\}+\left[\int_0^1\phi_i''\phi_j'' dx\right]\left\{\alpha_j\right\} = 0 \qquad (3.1)$$

In (3.1), for convenience, the same variables have been used to represent the motion about the equilibrium positions as in the original equations (2.30), (2.31) and (2.32).

3.2 Parametric Analysis

Parametric analysis is carried out based on (3.1) with the first mode of a cantilever beam as the basis function to simplify analysis.

Using only one basis function ϕ_1 and its corresponding coefficient function $\alpha_1(t)$, (3.1) is reduced to:

$$\begin{aligned}\ddot{p}+\omega_p^2 p &= 0\\ \ddot{q}+\omega_q^2 q+c_1\ddot{\alpha}_1+c_2\dot{\alpha}_1 &= 0\\ \ddot{\alpha}_1+\omega_1^2\alpha_1+c_3\ddot{q}+c_4\dot{\alpha}_1 &= 0\end{aligned} \qquad (3.2)$$

where c_1, c_2, c_3, c_4 and ω_1 are defined as:

$$\begin{aligned}c_1 &= \phi_1\big|_{x=s(t)} & c_2 &= \dot{s}\phi_1'\big|_{x=s(t)}\\ c_3 &= \frac{m\phi_1\big|_{x=s(t)}}{\int_0^1\phi_1^2dx+m\phi_1^2\big|_{x=s(t)}} & c_4 &= \frac{2m\dot{s}\phi_1\phi_1'\big|_{x=s(t)}}{\int_0^1\phi_1^2dx+m\phi_1^2\big|_{x=s(t)}}\\ \omega_1^2 &= \frac{m\ddot{s}\phi_1\phi_1'\big|_{x=s(t)}+m\dot{s}^2\phi_1\phi_1{}''\big|_{x=s(t)}+\int_0^1\phi_1''^2dx}{\int_0^1\phi_1^2dx+m\phi_1^2\big|_{x=s(t)}}\end{aligned} \qquad (3.3)$$

The characteristic equation is obtained by assuming:

$$\begin{aligned} p &= A_1 e^{i\Omega t} \\ q &= A_2 e^{i\Omega t} \\ \alpha_1 &= A_3 e^{i\Omega t} \end{aligned} \tag{3.4}$$

where A_1, A_2, A_3 and Ω are, in general, complex. Substituting (3.4) into (3.2), the following system of linear algebraic equations are obtained:

$$\begin{bmatrix} -\Omega^2 + \omega_p^2 & 0 & 0 \\ 0 & -\Omega^2 + \omega_q^2 & -c_1\Omega^2 + ic_2\Omega \\ 0 & -c_3\Omega^2 & ic_4\Omega + \omega_1^2 - \Omega^2 \end{bmatrix} \begin{Bmatrix} A_1 \\ A_2 \\ A_3 \end{Bmatrix} = \begin{Bmatrix} 0 \\ 0 \\ 0 \end{Bmatrix} \tag{3.5}$$

The characteristic equation of the system derived from (3.5) is given by:

$$(\Omega^2 - \omega_p^2)[(1 - c_3c_1)\Omega^4 + i(-c_4 + c_3c_2)\Omega^3 + (-\omega_1^2 - \omega_q^2)\Omega^2 + ic_4\omega_q^2\Omega + \omega_1^2\omega_q^2] = 0 \tag{3.6}$$

The positive roots of (3.6) are the natural frequencies of the linearized system, which are denoted as Ω_i. It can be seen from (3.6) that one of the natural frequencies equals to ω_p. Let this frequency be denoted by Ω_1. The second factor of (3.6) is a fourth order polynomial with complex coefficients and is therefore solved numerically. The four roots are in fact two complex roots Ω_2 and Ω_3, and their respective conjugates. It can be seen from (3.3) and (3.6) that Ω_2 and Ω_3 are influenced by the position, velocity and acceleration of the cart, $s(t), \dot{s}(t)$ and $\ddot{s}(t)$, mass m and ω_q. The variation in the roots with these parameters is investigated next.

The motion of the cart is assumed to be prescribed by the time histories shown in Figure 3.1. Starting from the fixed end of the beam to the free end, the cart accelerates first, next there is a constant velocity phase followed by deceleration until the velocity becomes zero at the free end. The length of the beam is assumed to be 1 in all the simulations.

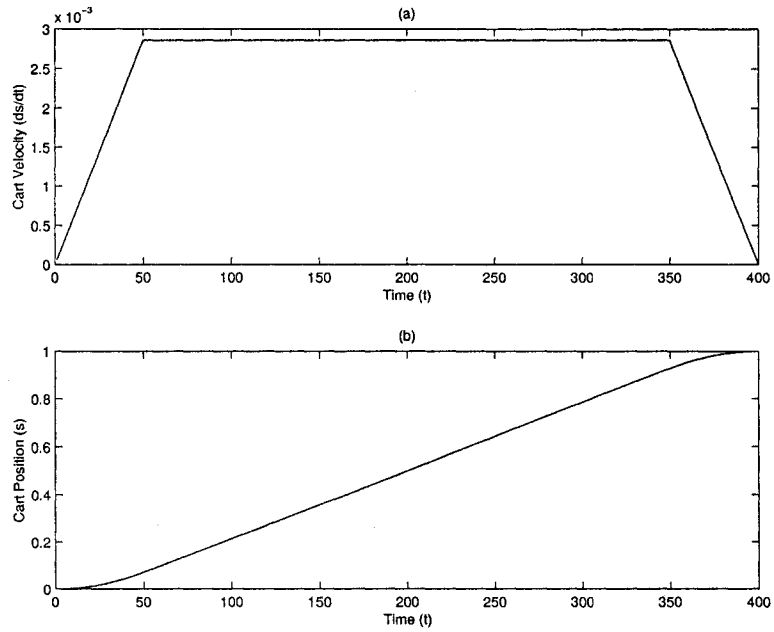

Figure 3.1: Prescribed cart motion. (a) $\dot{s}(t)$ - t, (b) $s(t)$ - t.

To implement the vibration suppression strategy, the natural frequencies Ω_1, Ω_2 and Ω_3 have to be made commensuable. It can be seen from (3.6) that Ω_1 depends only on ω_p. By changing ω_p, Ω_1 can be tuned to any desired value. The natural frequencies Ω_2 and Ω_3 depend on a number of parameters ($s(t), \dot{s}(t)$, $\ddot{s}(t)$, m and ω_q). The variation of natural frequencies Ω_2 and Ω_3 at $t = 150$ is shown in Figure 3.2(a) and that at $t = 350$ in Figure 3.2(b).

The vibration suppression strategy used in this work is to make Ω_2 and Ω_3 commensuable by tuning ω_q.

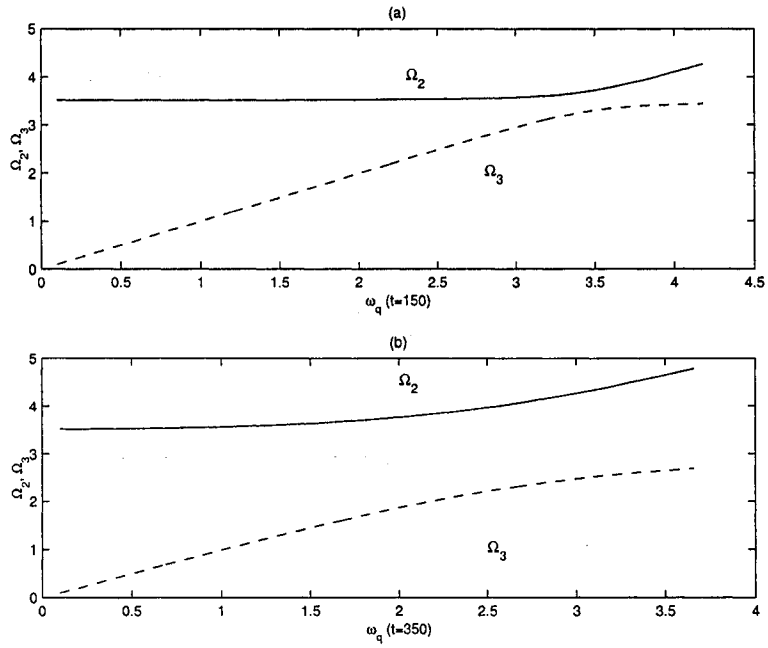

Figure 3.2: Linear natural frequencies Ω_2, Ω_3 variation with the tuning parameter ω_q, $m = 0.1$. (a)At $t = 150$, Ω_2, Ω_3 - ω_q, (b) At $t = 350$, Ω_2, Ω_3 - ω_q.

The equations of motion (2.30)- (2.32) show that p and α_1 are coupled through quadratic nonlinearities, and q and α_1 are linearly coupled. For such a case, it can be shown ([47] and [48]) that the frequency ratios $\Omega_1 \approx 2\Omega_3$ and $\Omega_2 \approx \Omega_3$ can result in internal resonance. The natural frequency Ω_1 can be approximately tuned to be equal to $2\Omega_3$ by setting $\omega_p = 2\Omega_3$.

Denoting the difference between Ω_2 and Ω_3 at any time instant as σ, to satisfy $\Omega_2 \approx \Omega_3$, we need to tune ω_q to make σ as small as possible. In some instances, it is possible to tune the system such that σ is zero. Such a case would correspond to

perfect 1 : 1 resonance. However, in general, the parametric space is such that it is not possible to tune σ to zero (example, Figure 3.2). The vibration suppression strategy requires that σ be made as small as possible. When σ is beyond a certain limit, the system goes out of internal resonance. A method to find the region of σ in which internal resonance exists was presented in [40]. To establish internal resonance between Ω_2 and Ω_3, ω_q is selected such that σ has the minimum possible value at every $s(t)$. The smallest possible σ depends on $s(t)$, $\ddot{s}(t)$ and m.

Tuning curves corresponding to the minimum value σ are obtained to establish internal resonance in the system. For the case when the cart with the prescribed motion shown in Figure 3.1, the tuning curves corresponding to the minimum value of σ is shown in Figure 3.3(a). When ω_q is tuned according to Figure 3.3(a), the natural frequencies Ω_2 and Ω_3 are as shown in Figure 3.3(b). The gap between these frequencies, which is the minimum possible σ, is shown in Figure 3.3(b). The smaller is the gap, the better satisfaction could be obtained in the internal resonance condition.

The effect of mass m on the tuning parameter ω_q is shown in Figure 3.4(a). This figure was obtained for the particular instant when the cart is at $s = 0.9$. The frequencies Ω_2 and Ω_3 corresponding to the tuning curve are shown in Figure 3.4(b) and the gap between these frequencies is shown in Figure 3.4(c). It can be seen from this figure that increasing mass increases the minimum gap between Ω_2 and Ω_3. Nevertheless, when the system is tuned according to the given tuned curve, the proposed vibration suppression strategy still works.

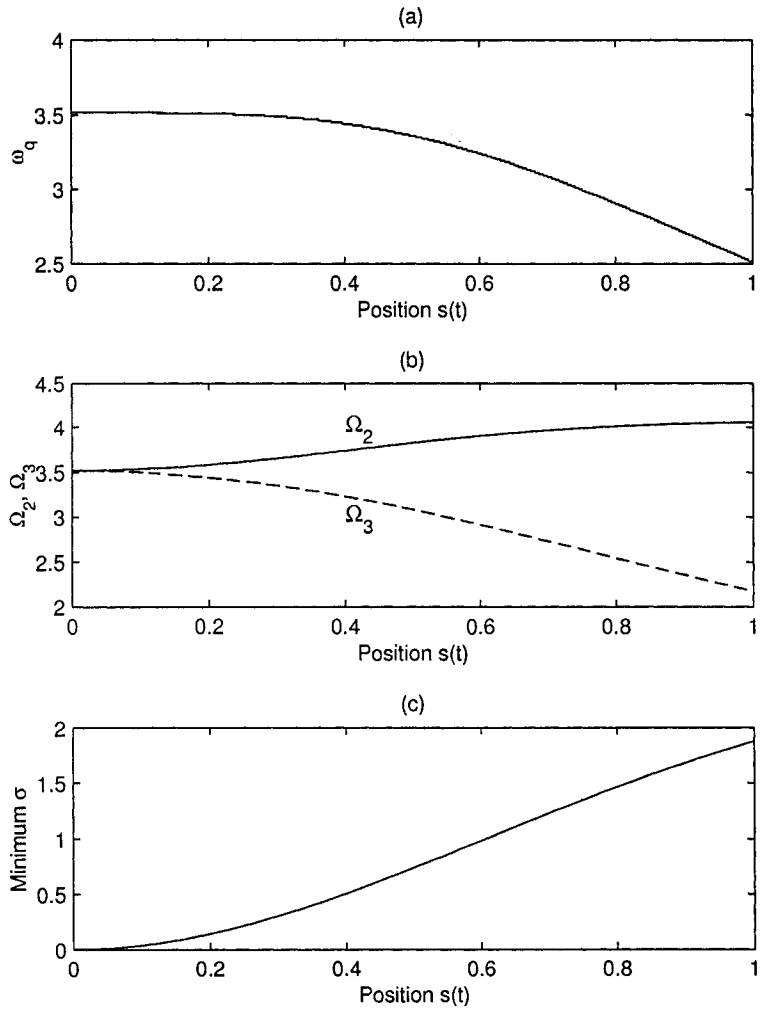

Figure 3.3: Tuning parameter ω_q, natural frequencies Ω_2, Ω_3 and the minimum gap σ variation with the position of the cart $s(t)$, $m = 0.1$. (a) ω_q - $s(t)$, (b) Ω_2, Ω_3 - $s(t)$, (c) σ - $s(t)$.

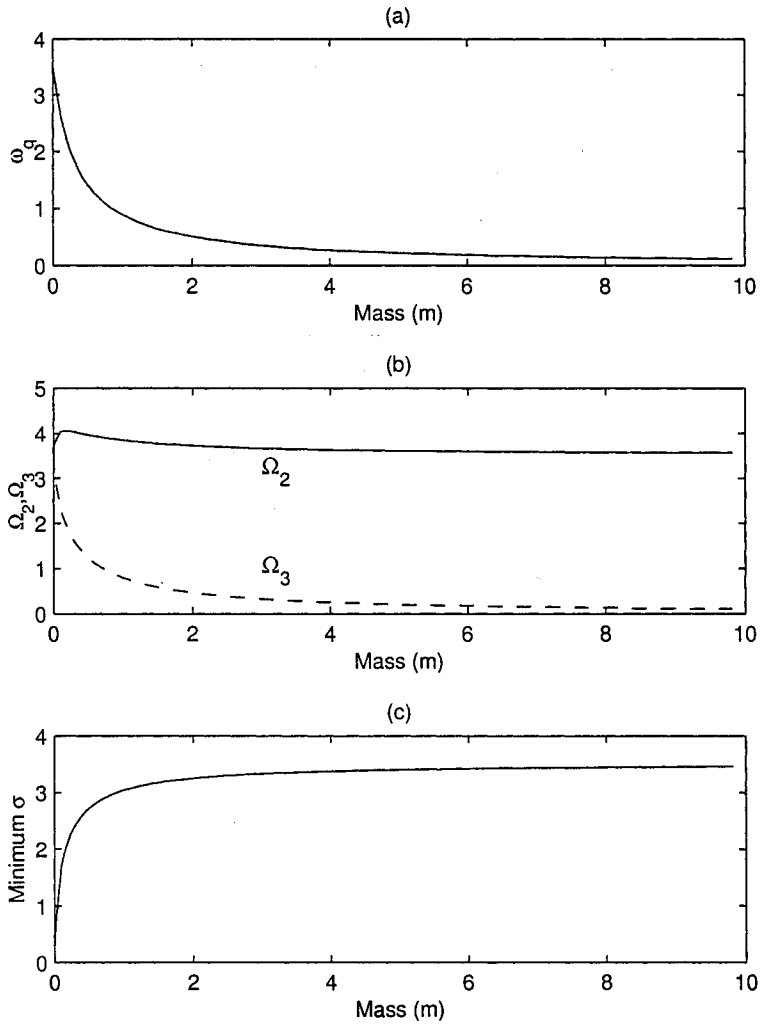

Figure 3.4: Tuning parameter ω_q, natural frequencies Ω_2, Ω_3 and the minimum gap σ variation with mass m at the position of the cart $s = 0.9$. (a) ω_q - m, (b) Ω_2, Ω_3 - m, (c) σ - m.

To investigate the influence of $\ddot{s}(t)$ on the natural frequencies of the system, the cart is assumed to move from the fixed end of the beam with a constant negative acceleration and an initial velocity such that the velocity becomes zero at the free end. The position and the velocity are shown in Figure 3.5. The tuned Ω_2, Ω_3, the corresponding σ, and the tuning parameter ω_q, when $\ddot{s}(t)$ varies from -0.0408 to -0.000012074 with $m = 0.1$ is shown in Figure 3.6. The acceleration $\ddot{s}(t)$ varying from -0.0408 to -0.000012074 corresponds to a variation of the total traveling time of the cart from 7 to 407. Figure 3.6 shows an instant when the cart position is $s = 0.9$. It can be seen from Figure 3.6 that acceleration has very little influence on the tuning parameter ω_q, the system frequencies Ω_2, Ω_3 and the minimum σ.

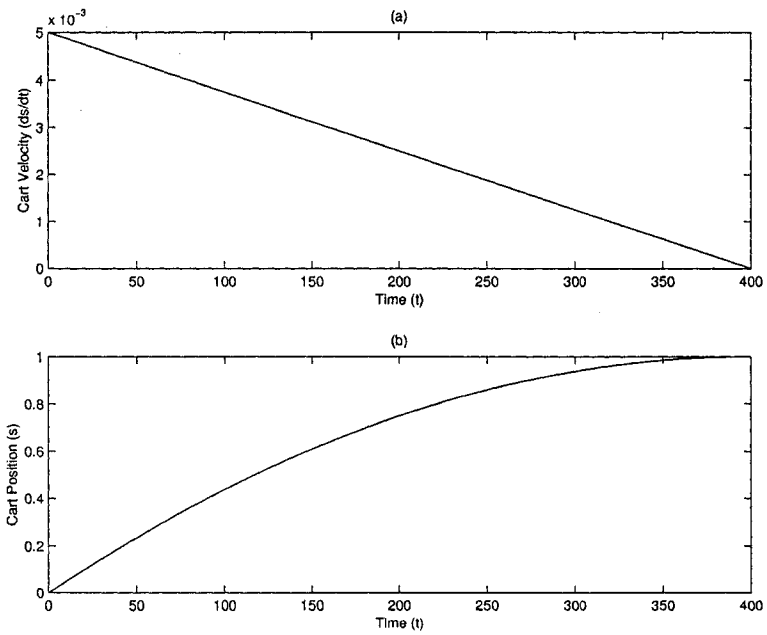

Figure 3.5: Cart motion with only negative acceleration. (a) $\dot{s}(t)$ - t, (b) $s(t)$ - t.

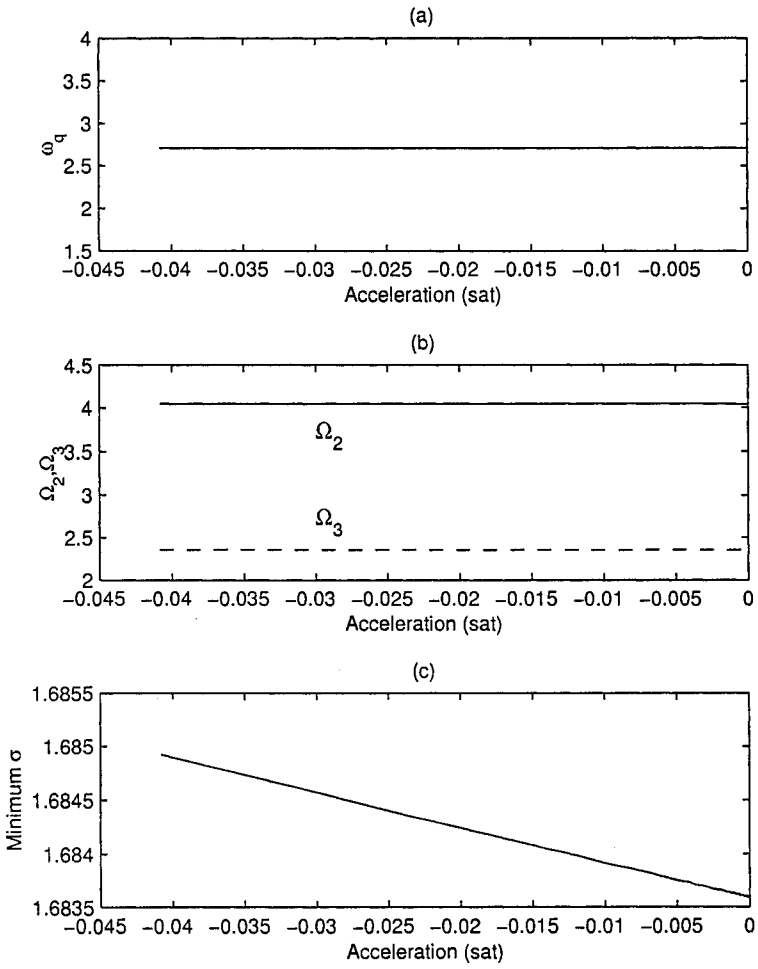

Figure 3.6: Tuning parameter ω_q, natural frequencies Ω_2, Ω_3 and the minimum gap σ variation with the cart's acceleration $\ddot{s}(t)$ at the position of the cart $s = 0.9$, $m = 0.1$. (a) ω_q - $\ddot{s}(t)$, (b) Ω_2, Ω_3 - $\ddot{s}(t)$, (c) σ - $\ddot{s}(t)$.

3.3 Implementation of Vibration Suppression Strategy

As mentioned in previous section, ω_p and ω_q needs to be tuned to satisfy $\Omega_1 \approx 2\Omega_3$ and ω_q need to be tuned to satisfy $\Omega_2 \approx \Omega_3$ to establish internal resonance in the system. The tuning curves for ω_q were presented in Section 3.2 and ω_p is set equal to $2\Omega_3$. The tuning of the frequencies is accomplished using position feedback of the form $T_p = -K_p p$ and $T_q = -K_q q$ in (2.30) and (2.31), respectively, and adjusting the position feedback gains K_p and K_q to make $\omega_p^2 - K_p$ and $\omega_q^2 - K_q$ resonate. Thus, the equations of motion are given by:

p equation:

$$\begin{aligned} &\ddot{p} + K_{dp}\dot{p} + \ddot{s} + (\omega_p^2 - K_p)p + \omega_p^2 p_e \\ &+\dot{s}\left\lfloor \phi_i\phi_j'' + \phi_i'\phi_j' \right\rfloor_{x=s(t)} \{\dot{\alpha}_i\alpha_j\} + \left\lfloor \phi_i\phi_j' \right\rfloor_{x=s(t)} \{\dot{\alpha}_i\dot{\alpha}_j + \ddot{\alpha}_i\alpha_j\} \;=\; 0 \end{aligned} \tag{3.7}$$

q equation:

$$\begin{aligned} &\ddot{q} + K_{dq}\dot{q} + (\omega_q^2 - K_q)q + \omega_q^2 q_e \\ &+\dot{s}\left\lfloor \phi_i' \right\rfloor_{x=s(t)} \{\dot{\alpha}_i\} + \left\lfloor \phi_i \right\rfloor_{x=s(t)} \{\ddot{\alpha}_i\} \;=\; 0 \end{aligned} \tag{3.8}$$

v equation:

$$\begin{aligned} &m\Big\{ \left[\phi_i\phi_j\right]_{x=s(t)} \{\ddot{\alpha}_j\} + \ddot{q}\left\{\phi_i\right\}_{x=s(t)} \\ &+ \left[\phi_i\phi_j'\right]_{x=s(t)} \{(\ddot{p} + \ddot{s})\{\alpha_j\} + (2\dot{s} + \dot{p})\{\dot{\alpha}_j\}\} \end{aligned}$$

$$+(\dot{s}\dot{p}+\dot{s}^2)\left[\phi_i\phi_j''\right]_{x=s(t)}\{\alpha_j\}\Big\}$$
$$+\left[\int_0^1 \phi_i\phi_j dx\right]\{\ddot{\alpha}_j\}+\left[\int_0^1 \phi_i''\phi_j'' dx\right]\{\alpha_j\} = 0 \quad (3.9)$$

where K_{dp} and K_{dq} are velocity feedback gains which are discussed next. When the system is tuned under internal resonance, damping is introduced in p and q directions using velocity feedback to suppress vibration in the system. This can be considered as a D controller. Velocity feedback is represented by $K_{dp}\dot{p}$ and $K_{dq}\dot{q}$ in (3.7) and (3.8), where K_{dp} and K_{dq} can be tuned to achieve best vibration suppression result. In general, increasing K_{dp} and K_{dq} up to a certain limit reduces the settling time. This limit depends on system parameters and finding them analytically is a challenging task. In this work we use trial and error to adjust K_{dp} and K_{dq} to obtain a reasonable settling time.

In order to implement the vibration suppression strategy, a tunable PD controller is needed in p and q directions for position and velocity feedback. The controller in p direction can also be used for implementing the prescribed cart motion. A conceptual control logic diagram is shown in Figure 3.7.

The prescribed motion of the traversing cart, s, $\dot{s}$ and $\ddot{s}$, is the input to the system. Using the method outlined in Section 3.2, the tuning parameter ω_q and the natural frequencies Ω_2 and Ω_3 are determined. Block 1 indicates the computation of the controller gain K_p based on minimization of the difference between Ω_1 and $2\Omega_3$. Block 2 indicates the position and the velocity feedback to establish internal resonance and introduce damping in the system in the p mode. Block 3 describes the computation of the controller gain K_q based on the minimization of the difference

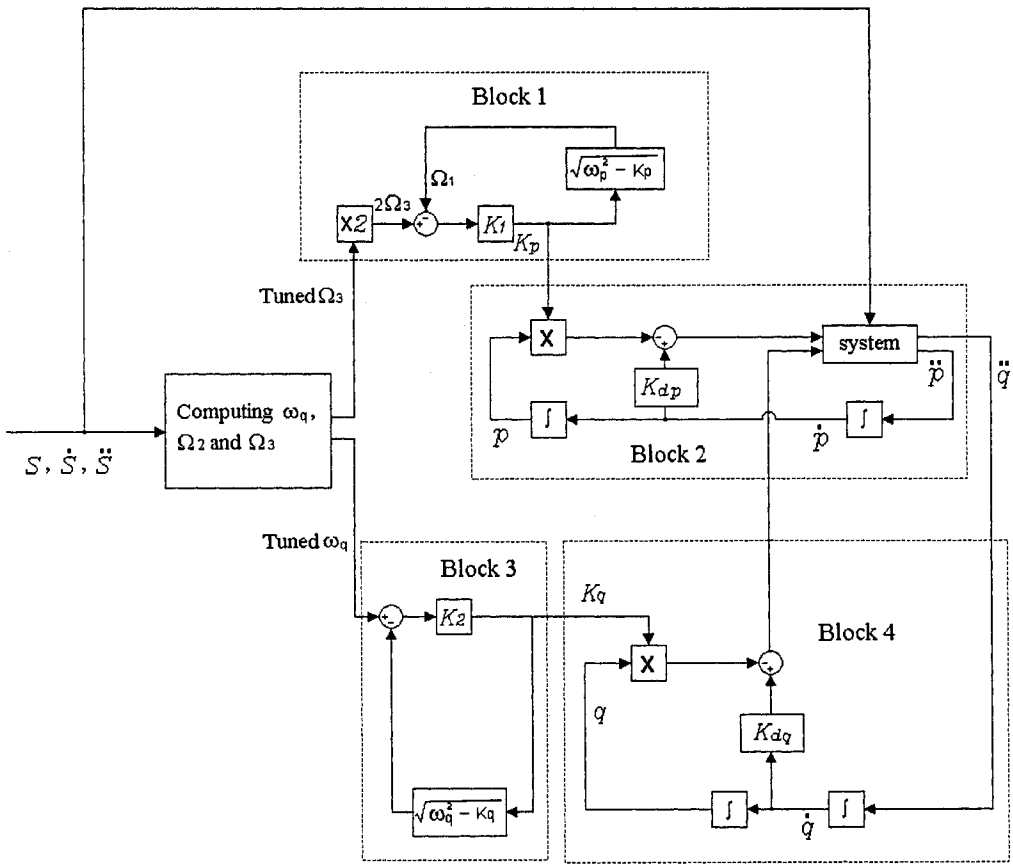

Figure 3.7: Conceptual control logic, K_1 and K_2 are gains for tuning K_p and K_q.

between Ω_2 and Ω_3 through the tuning parameter ω_q. Block 4 indicates the position and the velocity feedback to the q mode for establishing internal resonance between q and the first mode of the beam and introducing damping in the q mode for vibration suppression. This control strategy can be further improved by computing natural frequencies and tuning parameters from system feedback rather than using the theoretical values. This is left as future work.

In this chapter, linear natural frequencies of the system were analyzed to obtain tuning curves to establish internal resonance and the vibration suppression strategy was presented. In the next chapter, dynamics of the beam carrying spring-mass system is investigated numerically and system response is analyzed.

Chapter 4

System Response Analysis

In this chapter, dynamics of the system is investigated numerically. The vibration suppression strategy described in Chapter 3 is established numerically and dynamics of the system studied using spectral analysis techniques.

4.1 Numerical Solution

The equations of motion (3.7)-(3.9) are solved numerically using four cantilever beam mode shapes (2.33) as basis functions to obtain system response. The Adaptive Stepsize Runge-Kutta Method discussed in Section 1.4.2 is used for obtaining the solution.

4.2 Spectral Analysis

System response is analyzed in spectral domain using power spectrum and time-frequency analysis. For power spectrum analysis, the numerical solution obtained need to be interpolated to make the data step size constant. Cubic polynomial interpolation is used. Next, power spectrum is obtained by applying the Hann window to the data segment and finding its one sided Power Spectral Density(PSD), with mean squared amplitude as the measure, by the Fast-Fourier transform (FFT) algorithm [45]. To reduce the variance, data points are segmented and overlapped. The computed FFTs are averaged.

4.3 Resonant and Non-Resonant Response

In all the simulations presented in this section, the cart is assumed to move with the prescribed motion shown in Figure 4.1, which is the same as Figure 3.1, repeated here for convenience. Parameters used in simulations are shown in Table 4.1.

Parameter Sets $m = 1$, $p_e = 0$, $q_e = 0$						
No.	K_{dp}	K_{dq}	v_{t0}	p_0	q_0	Figure
1			0.1	0.00001	0.00001	4.2-4.10
2	0.3	0.3	0.1	0.00001	0.00001	4.16-4.20
3			0.00001	0.00001	0.1	4.11- 4.15
4	0.3	0.9	0.00001	0.00001	0.1	4.21- 4.25

Table 4.1: Parameter sets.

The coupling between the moving mass and beam is, in general, weak. internal resonance is used for enhancing the coupling. Figure 4.2 shows a typical time

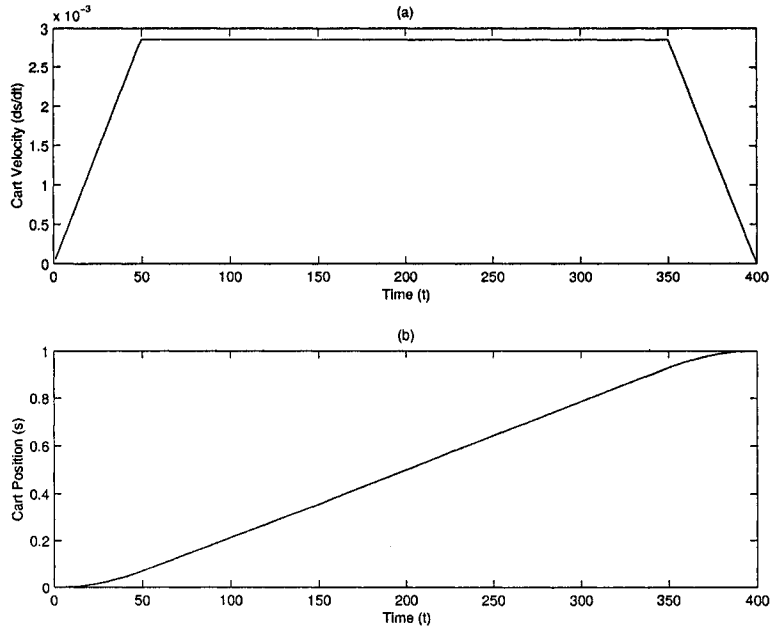

Figure 4.1: Prescribed cart motion. (a) $\dot{s}(t)$ - t, (b) $s(t)$ - t.

response when the parameters are as chosen that the system is away from internal resonance. In Figure 4.2, Parameter Set 1 in Table 4.1 is used and ω_p and ω_q are selected such that the frequencies are not in internal resonance. It can be seen from Figure 4.2 that coupling between the beam and moving mass is weak as indicated by little vibration of $p(t)$ and $q(t)$. When system parameters satisfy internal resonance conditions, the coupling between the beam and moving mass becomes strong. This strong coupling can then be used to transfer energy from one subsystem to another. By adding damping to the moving mass when the system is under internal resonance, vibration of the beam and moving mass can be suppressed. Figure 4.3 shows a resonant case, where ω_q is continuously tuned so that $\Omega_2 \approx \Omega_3$ and ω_p is selected to be equal to $2\Omega_3$. For this case, Parameter Set 1

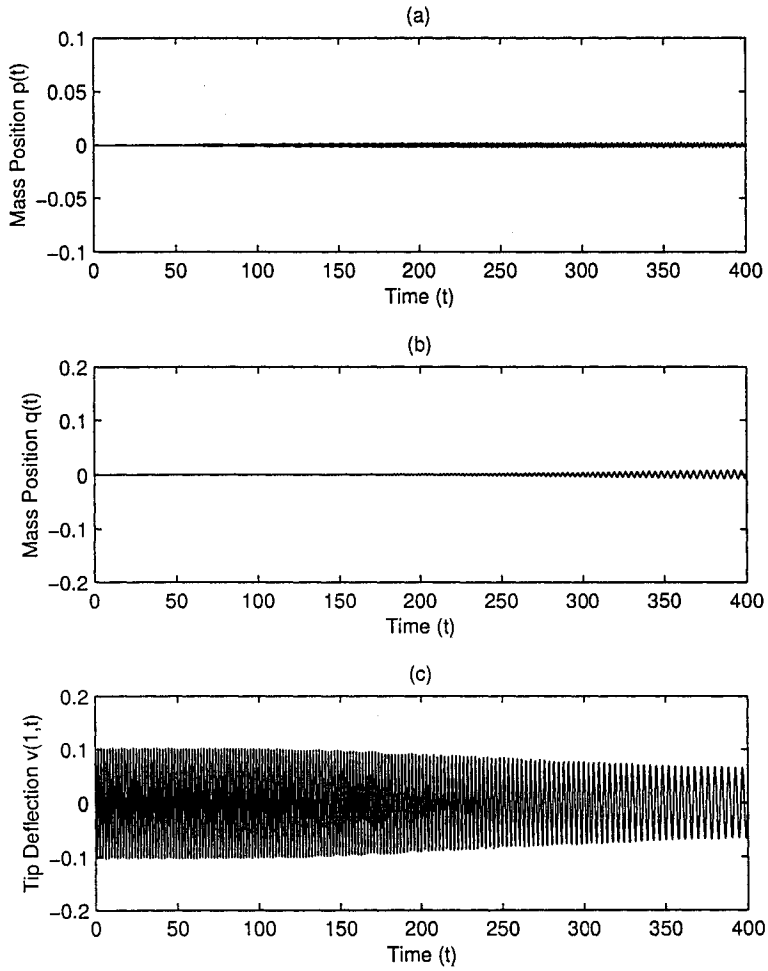

Figure 4.2: System response without internal resonance, $m = 1$, $v_{t0} = 0.1$, $p_0 = 0.00001$, $q_0 = 0.00001$. (a) the p mode of the mass, (b) the q mode of the mass, (c) Beam tip deflection.

(see Table 4.1) is used for simulation.

It can been seen from Figure 4.3 that when initial value is given to the beam, energy exists in the beam initially, then transfers to first the q mode and next the p mode of the mass. When the amplitude of q decreases, the amplitude of v_{t0} increases and energy goes back from the mass to the beam. Comparing Figure 4.2 with Figure 4.3, the effect of internal resonance can be clearly seen. Under internal resonance conditions, energy transfers back and forth between the beam and moving mass, resulting in very strong coupling. This is the key to the vibration suppression strategy in this work.

Figure 4.4 is the power spectrum for the system response shown in Figure 4.3. The FFTs are calculated with 32768 data points and the average time step for the data points is 0.00529. Figure 4.4(a) shows the power spectrum the p mode of the mass. In this case, major peaks appear near the even multiplies of Ω_3(eg. $2\Omega_3, 4\Omega_3, 6\Omega_3, \cdots$). These peaks are not at exact even multiplies of Ω_3, but are very close to the even multiplies. This is due to the fact that Ω_2 and Ω_3 are not in perfect internal resonance but there is a small detuning σ, which arises because the parameter space is such that it is not possible to tune Ω_2 and Ω_3 to be exactly the same. Figure 4.4(c) shows the power spectrum for the beam. The major peaks appear near the odd multiplies of Ω_3 ($\Omega_3, 3\Omega_3, 5\Omega_3, ...$), as these peaks approach the second and the third natural frequency of the beam (22.19 and 61.77, respectively), the energy in these peaks increases. It should also be noted that under internal resonance, the system response is predominantly bi-periodic. In other words, the response frequencies have the integral combination of the lowest natural frequency

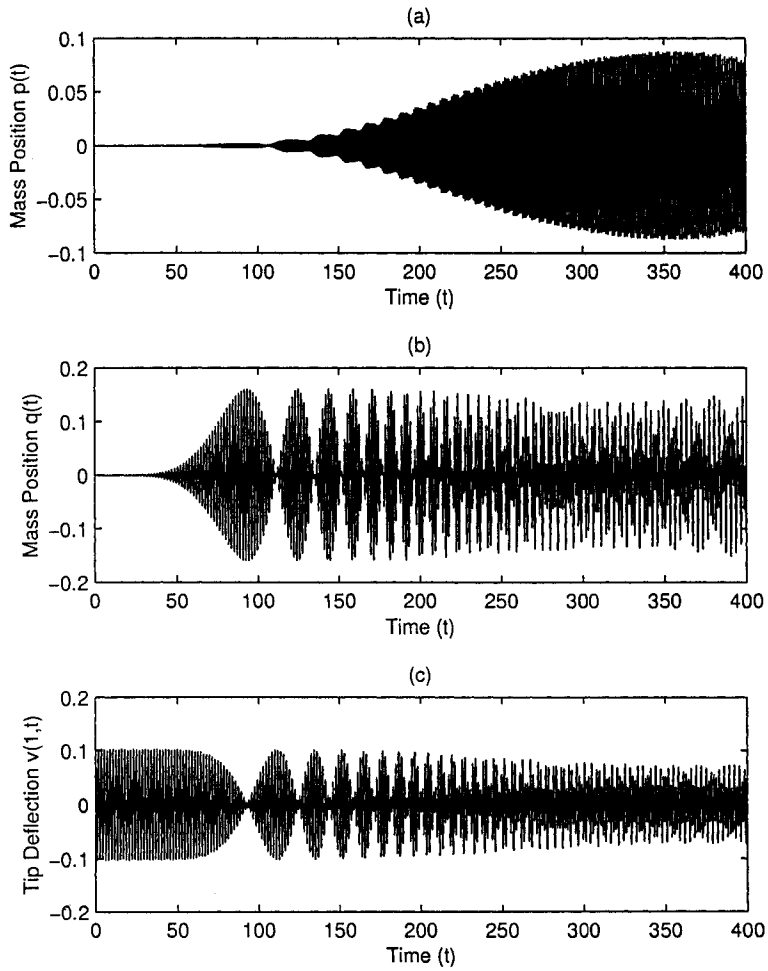

Figure 4.3: System response, $m = 1$, $v_{t0} = 0.1$, $p_0 = 0.00001$, $q_0 = 0.00001$. (a) the p mode of the mass, (b) the q mode of the mass, (c) Beam tip deflection.

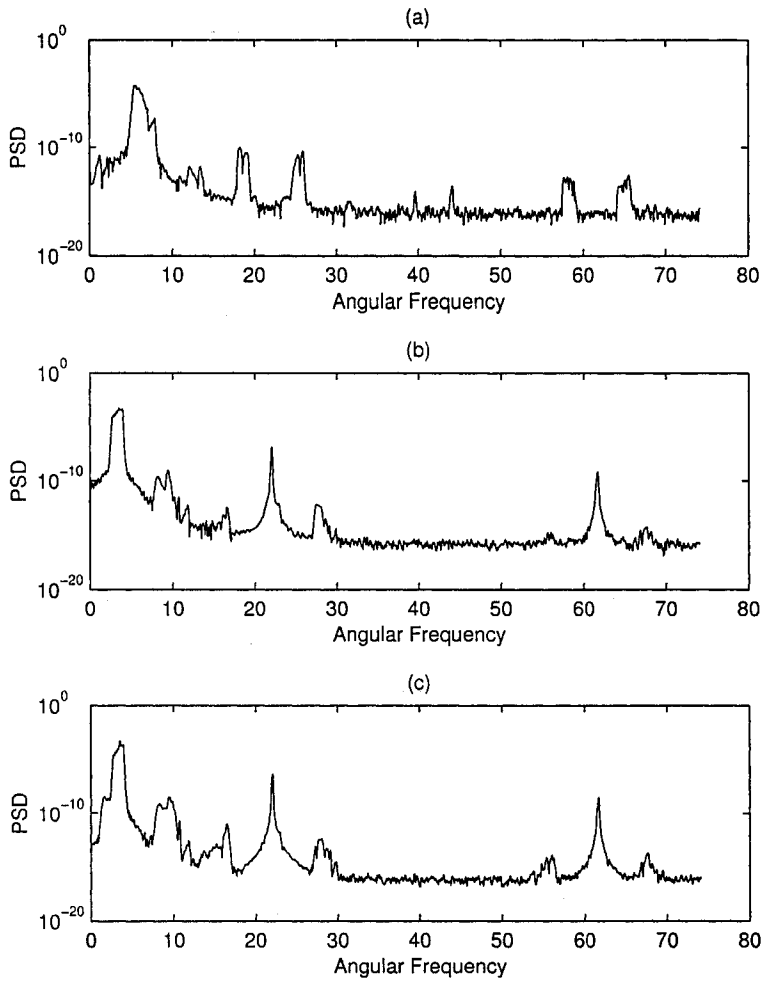

Figure 4.4: Power spectrum, $m = 1$, $v_{t0} = 0.1$, $p_0 = 0.00001$, $q_0 = 0.00001$. (a) the p mode of the mass, (b) the q mode of the mass, (c) Beam Tip deflection v_{t0}.

of the system and the beating frequency. This results in side bands in the power spectrum (Figure 4.4). Figure 4.4(b) is the spectrum for q mode of the mass, which is similar to Figure 4.4(c) because the q mode and the beam are linearly coupled.

It can been seen from Figure 4.4 that the peaks are not sharply defined. This is due to the fact that the system is time-varying and the averaging makes the peaks flatter. In order to investigate the time varying behavior of the response, time-frequency analysis is carried out.

Time-frequency spectrogram is obtained by finding power spectrum of relatively small segments of data and the results are displayed on time and frequency axes, with time corresponding to the center of the data segment shown on x axis and frequency shown on y axis. The power spectral density is shown using grey scaling for the whole plot. Dark shades represent higher energy level compared to ligher shades (reference Figure 4.6). For smoother transitions, the data segments are overlapped.

As the cart moves along the length of the beam, the natural frequencies change. This change in the frequencies can be seen clearly in the spectrograms shown in Figures 4.5-4.8. As the cart moves from one end to the other, the separation of the side bands also increases. To further investigate transfer of energy under internal resonance conditions, the frequency bands are magnified as shown in Figure 4.9 and Figure 4.10. Figure 4.9 is obtained for the q mode of the mass and Figure 4.10 for the tip deflection of the beam. The magnified spectrograms clearly show the changing energy content of the frequencies. It can be seen clearly from Figure 4.9, that when q reaches amplitude crest, energy in the fundamental natural frequency

in the q mode increases.

4.4 Comparison of Different Excitation Modes

Next, we compare the effect of excitation in different modes. The previous simulations, Figures 4.3-4.10, were based on the initial value given to the beam. Figures 4.11-4.15 show the case where the initial value is given to the q mode of the moving mass. Since in this case, the system is excited by a single frequency subsystem (as opposed to the beam excitation where there is contribution from higher modes), energy is mostly exchanged between the lower harmonics. This is indicated by the relative lack of higher energy in the high frequency band of the beam response in Figure 4.12(c).

Figure 4.11 shows system time response under internal resonance using Parameter Set 3 in Table 4.1. It can be seen that energy initially existing in the q mode of the mass first transfers to the beam and to the p mode of the mass and then back to the q mode due to internal resonance. Figure 4.12 is the power spectrum for the system response shown in Figure 4.11. Higher frequencies' energy is weak in this case, which is due to the fact the system is excited by a single frequency subsystem and energy is mostly exchanged between lower harmonics. Time frequency spectrograms (Figures 4.13-4.15) show this phenomenon more clearly.

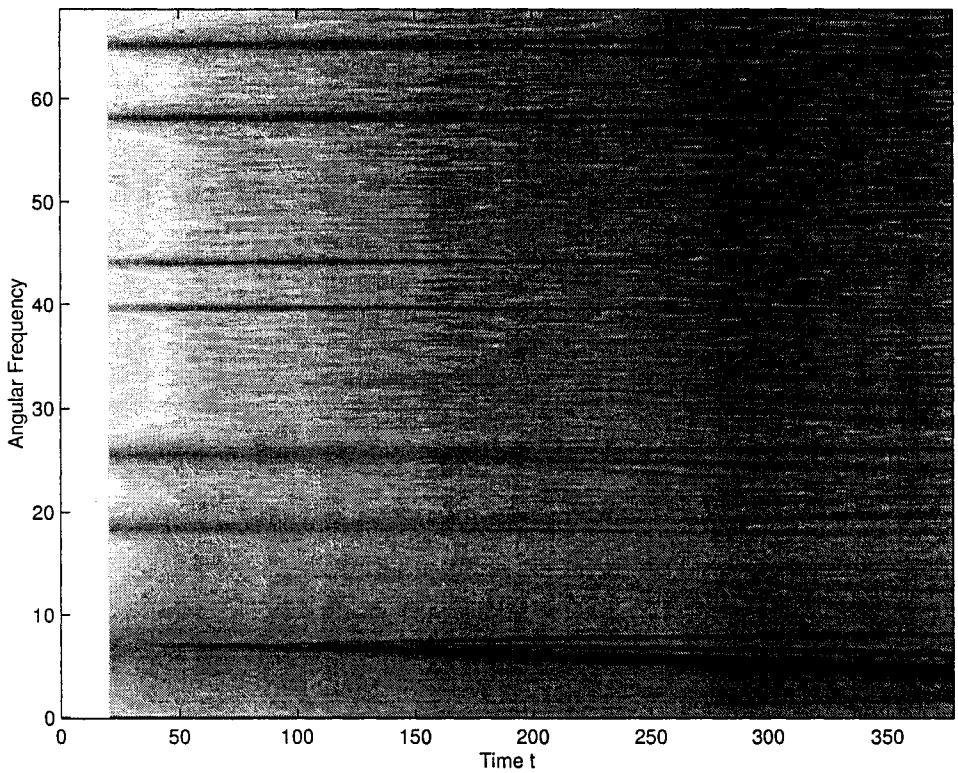

Figure 4.5: Spectrogram for the p mode of the mass, $m = 1$, $v_{t0} = 0.1$, $p_0 = 0.00001$, $q_0 = 0.00001$.

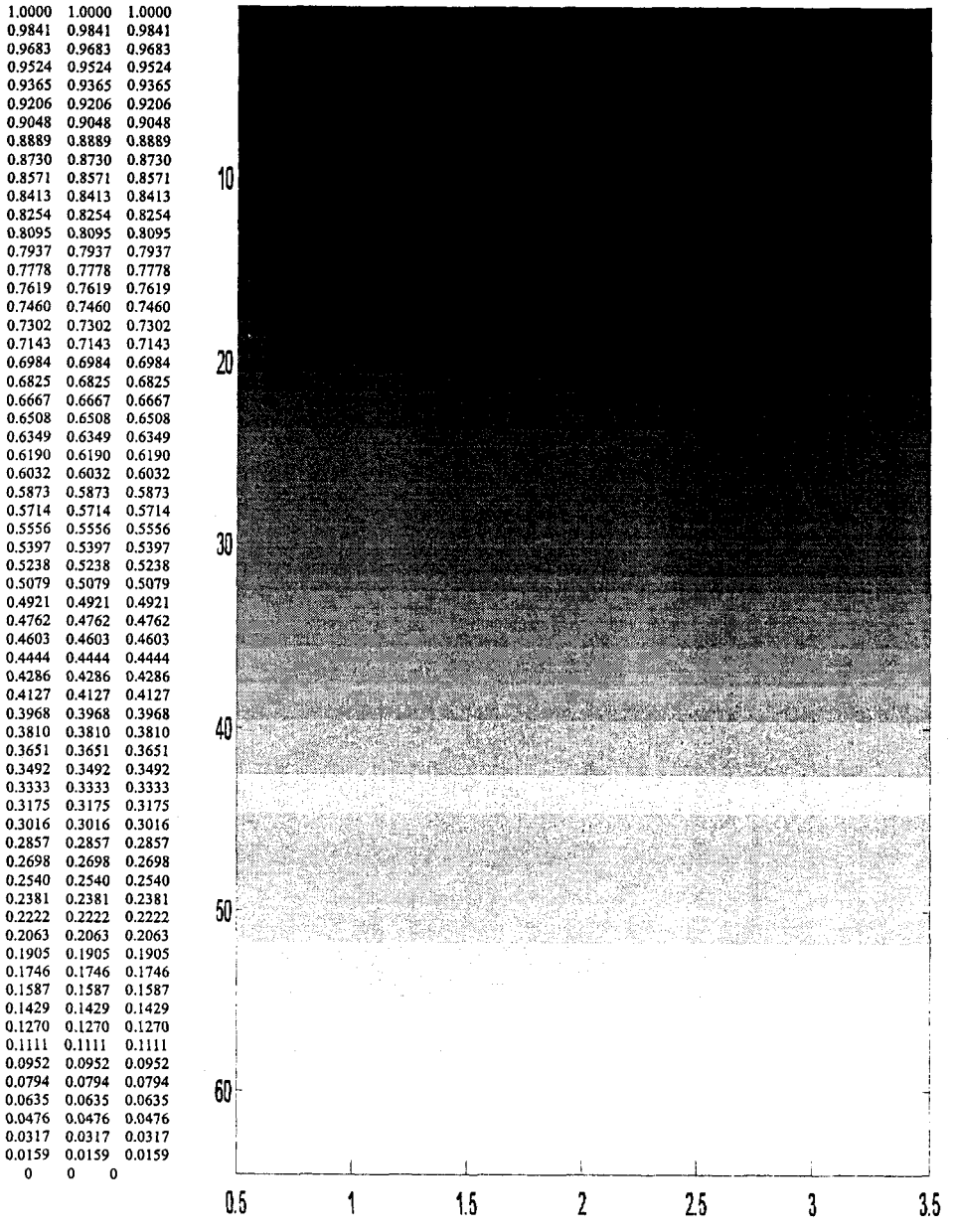

Figure 4.6: Gray level for spectrogram

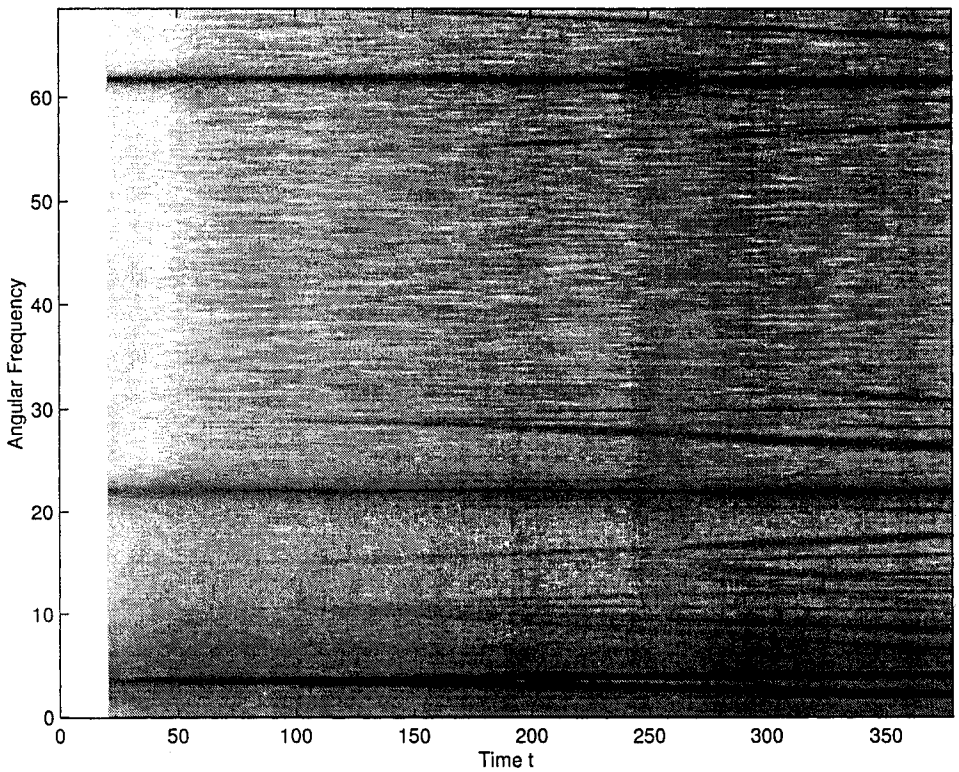

Figure 4.7: Spectrogram for the q mode of the mass, $m = 1$, $v_{t0} = 0.1$, $p_0 = 0.00001$, $q_0 = 0.00001$.

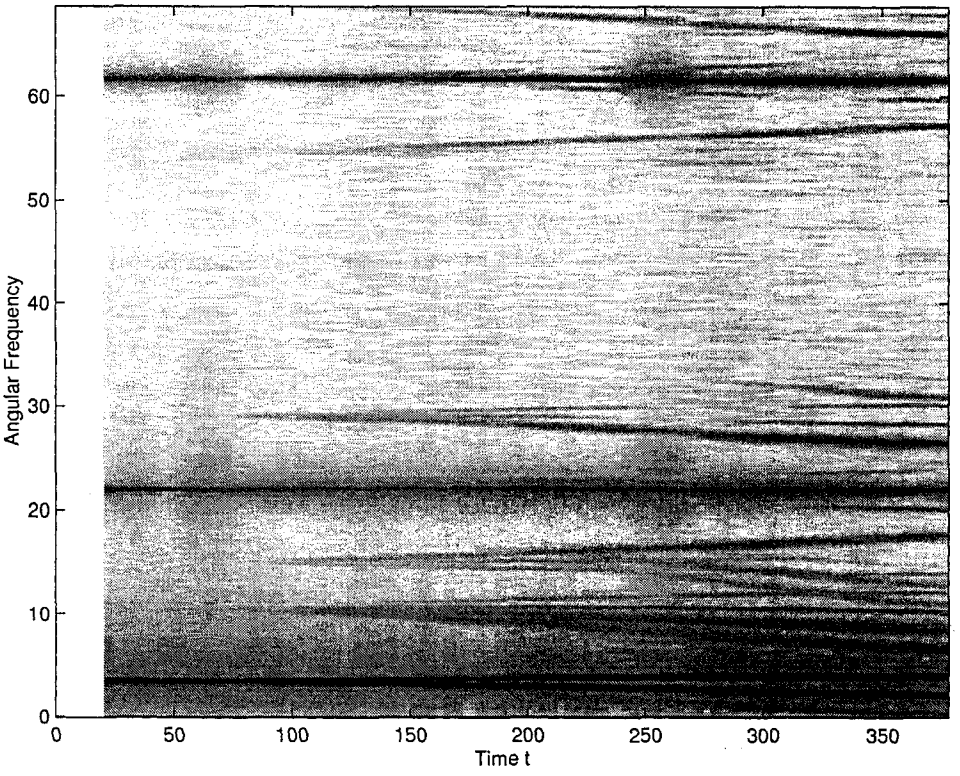

Figure 4.8: Spectrogram for beam tip deflection v_{t0}, $m = 1$, $v_{t0} = 0.1$, $p_0 = 0.00001$, $q_0 = 0.00001$.

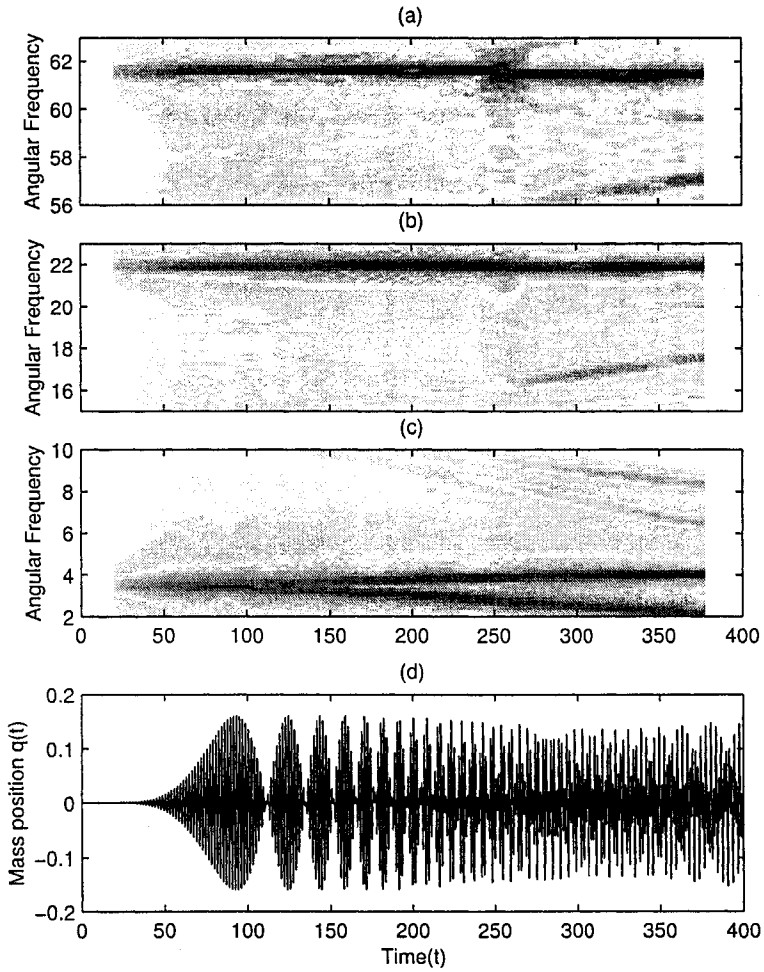

Figure 4.9: Magnified spectrogram for the q mode of the mass, $m = 1$, $v_{t0} = 0.1$, $p_0 = 0.00001$, $q_0 = 0.00001$.

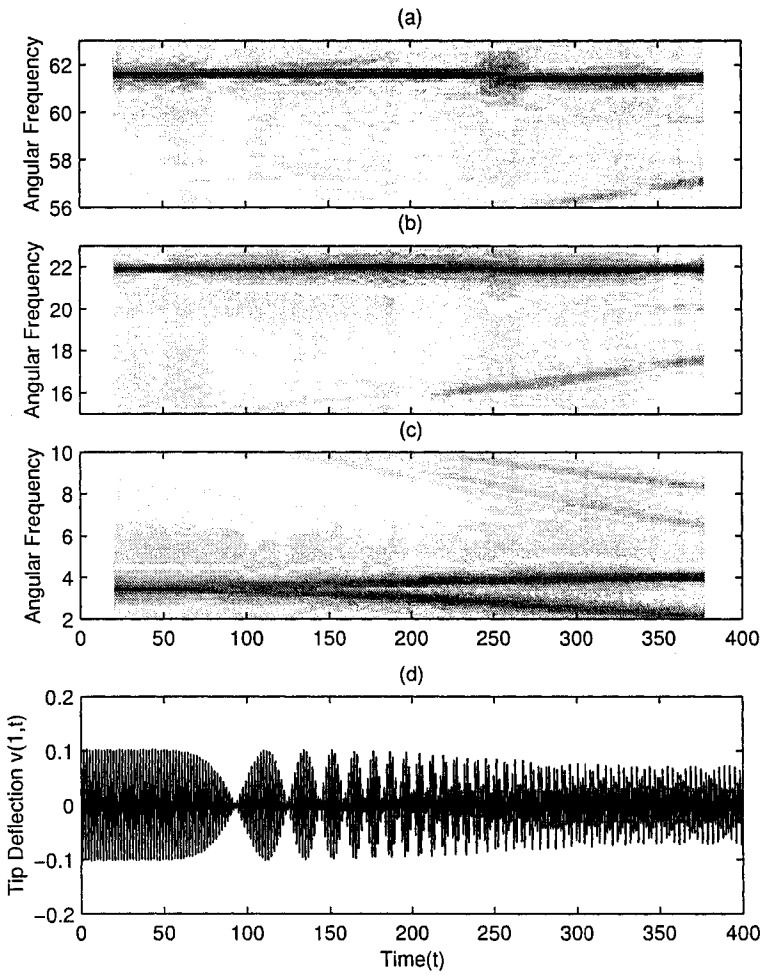

Figure 4.10: Magnified spectrogram for beam tip deflection v_{t0}, $m = 1$, $v_{t0} = 0.1$, $p_0 = 0.00001$, $q_0 = 0.00001$.

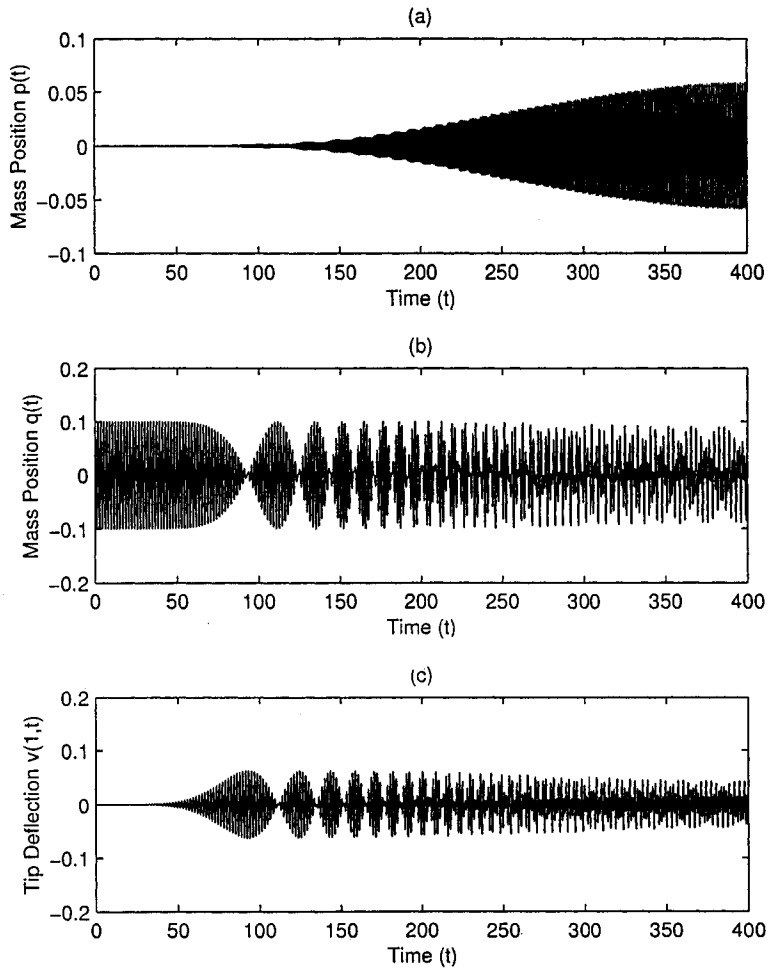

Figure 4.11: System response, $m = 1$, $v_{t0} = 0.00001$, $p_0 = 0.00001$, $q_0 = 0.1$. (a) the p mode of the mass, (b) the q mode of the mass, (c) Beam tip deflection.

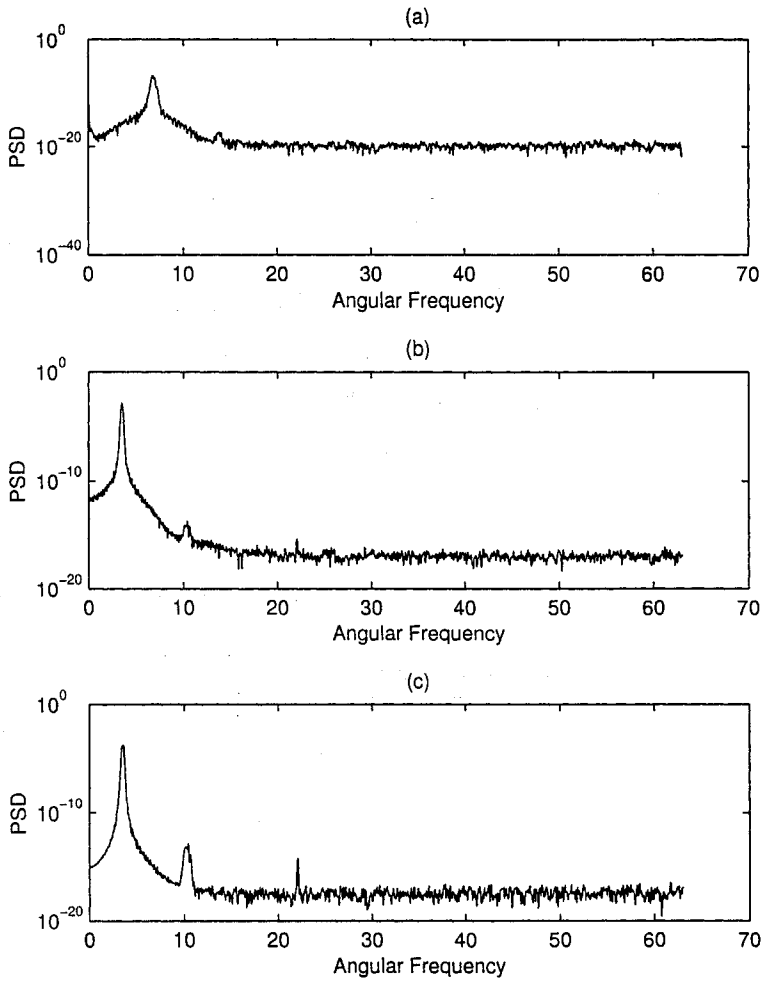

Figure 4.12: Power spectrum, $m = 1$, $v_{t0} = 0.00001$, $p_0 = 0.00001$, $q_0 = 0.1$ (a) the p mode of the mass, (b) the q mode of the mass, (c) Beam tip deflection.

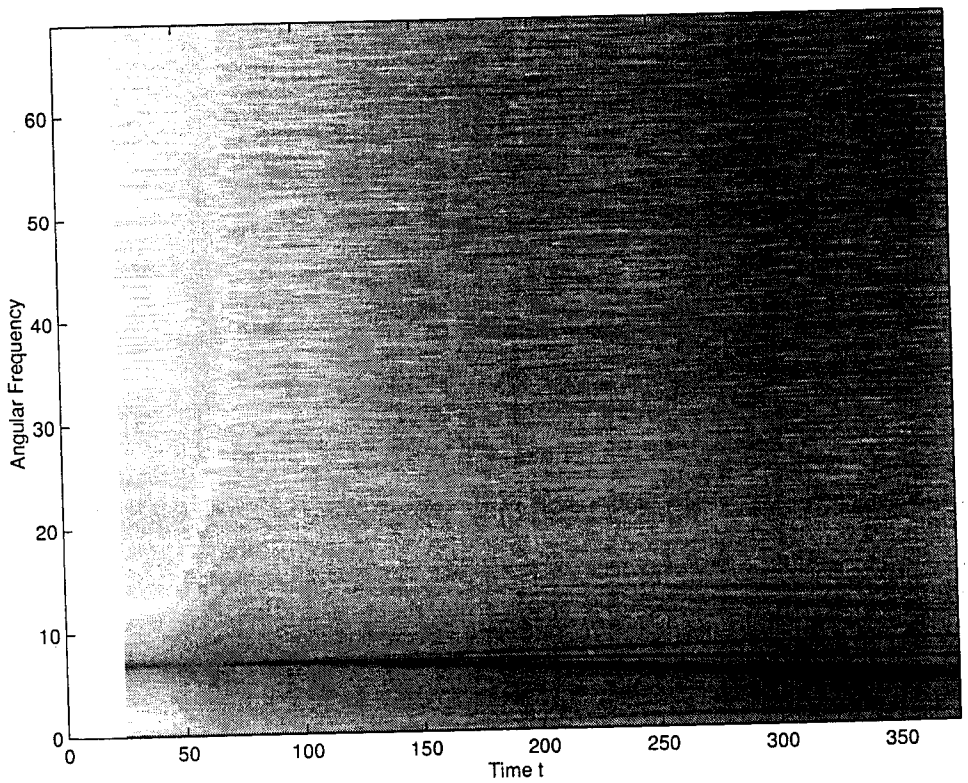

Figure 4.13: Spectrogram for the p mode of the mass, $m = 1$, $v_{t0} = 0.00001$, $p_0 = 0.00001$, $q_0 = 0.1$.

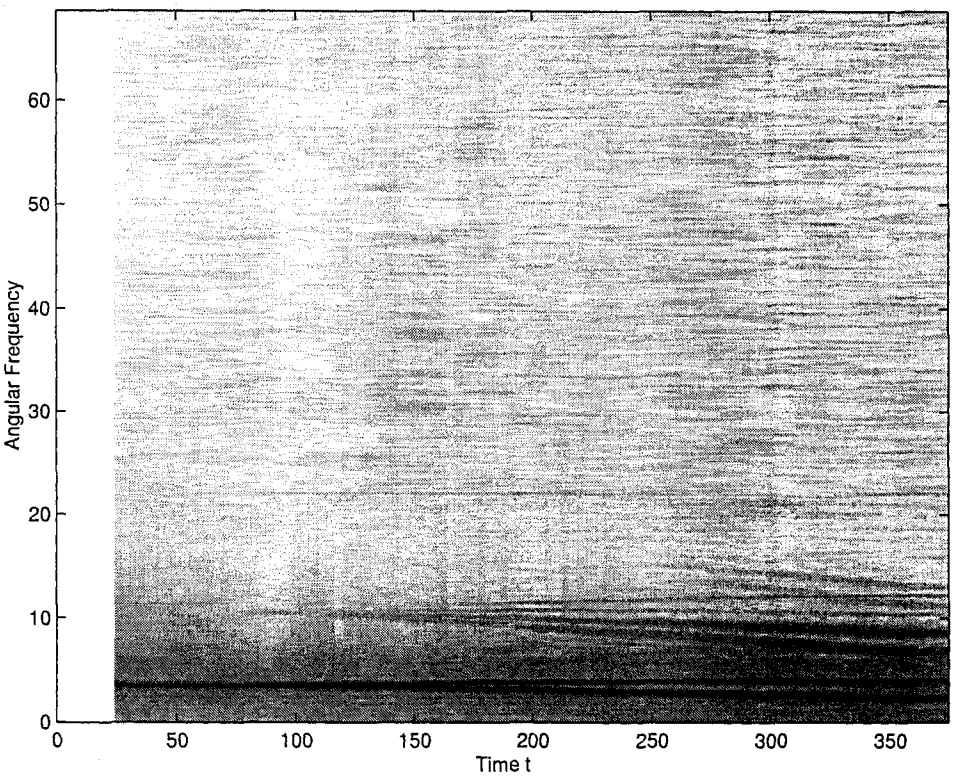

Figure 4.14: Spectrogram for the q mode of the mass, $m = 1$, $v_{t0} = 0.00001$, $p_0 = 0.00001$, $q_0 = 0.1$.

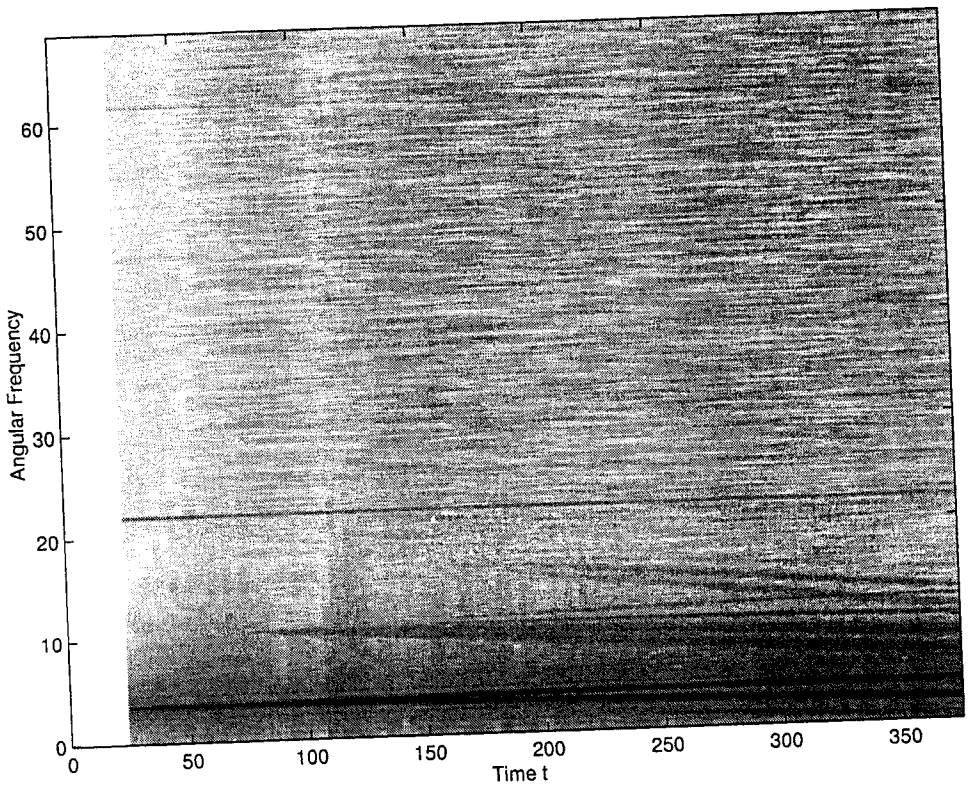

Figure 4.15: Spectrogram for beam tip deflection v_{t0}, $m = 1$, $v_{t0} = 0.00001$, $p_0 = 0.00001$, $q_0 = 0.1$.

4.5 Vibration Suppression

Once internal resonance is established, vibrations are suppressed by introducing damping in the moving mass modes. This not only suppresses vibrations in the moving mass, but also suppresses vibrations in the beam using the strong coupling which exists due to internal resonance. Simulations using the internal resonance based vibration suppression strategy are shown in Figures 4.16-4.20 for Parameter Set 2 (see Table 4.1). As it can be clearly seen from the time response shown in Figure 4.16, the vibrations of the beam and the moving mass are suppressed quickly. The settling time can be further reduced by increasing the damping. The system response for this case without damping were shown earlier in Figure 4.3.

The power spectrum for the system response is shown in Figure 4.17, where it can be seen the power spectral density of frequencies is much lower than that of the undamped response which was shown in Figure 4.4. The flat peaks are due to the fact the system is time variant and the power spectrum averages frequencies all the length of the time series. Time-frequency spectrograms shown in Figures 4.18-4.20 indicates the damping is most effective in the lower frequencies.

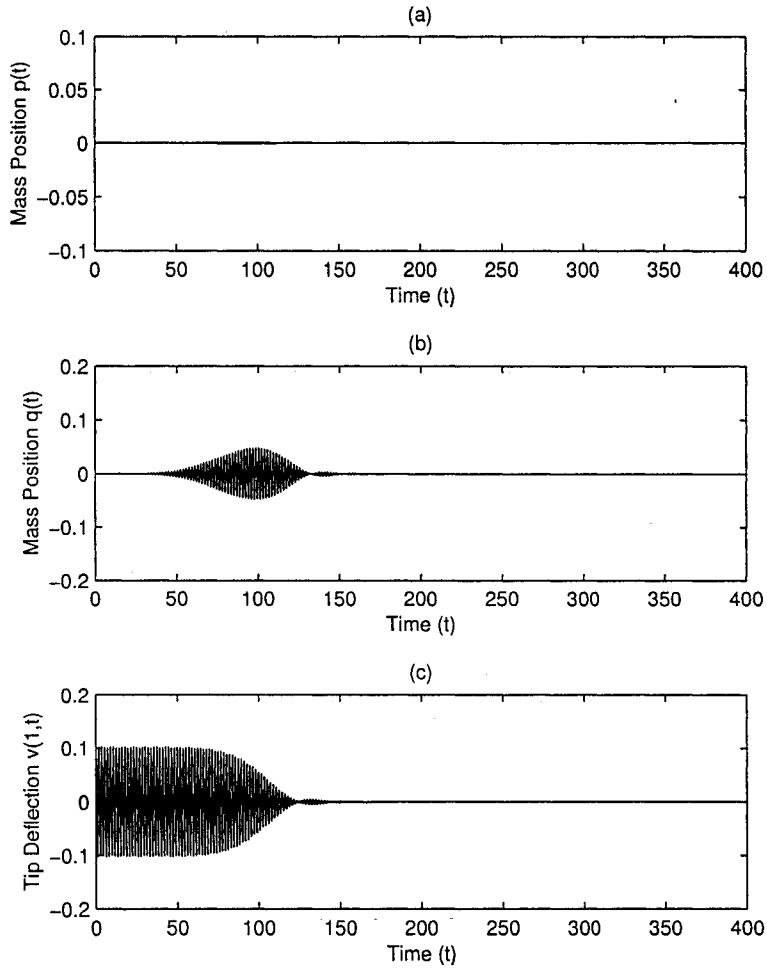

Figure 4.16: System response with damping, $m = 1$, $v_{t0} = 0.1$, $p_0 = 0.00001$, $q_0 = 0.00001$, $K_{dp} = 0.3$, $K_{dq} = 0.3$. (a) the p mode of the mass, (b) the q mode of the mass, (c) Beam tip deflection.

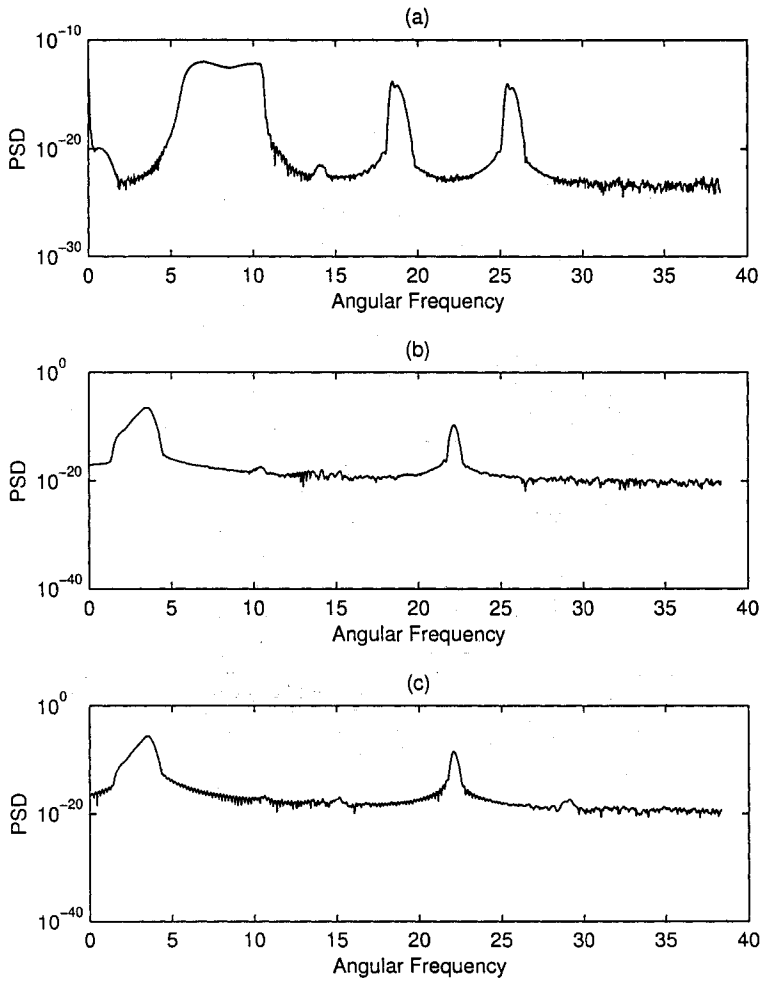

Figure 4.17: Power spectrum, $m = 1$, $v_{t0} = 0.1$, $p_0 = 0.00001$, $q_0 = 0.00001$, $K_{dp} = 0.3$, $K_{dq} = 0.3$.(a) the p mode of the mass, (b) the q mode of the mass, (c) Beam tip deflection v_{t0}.

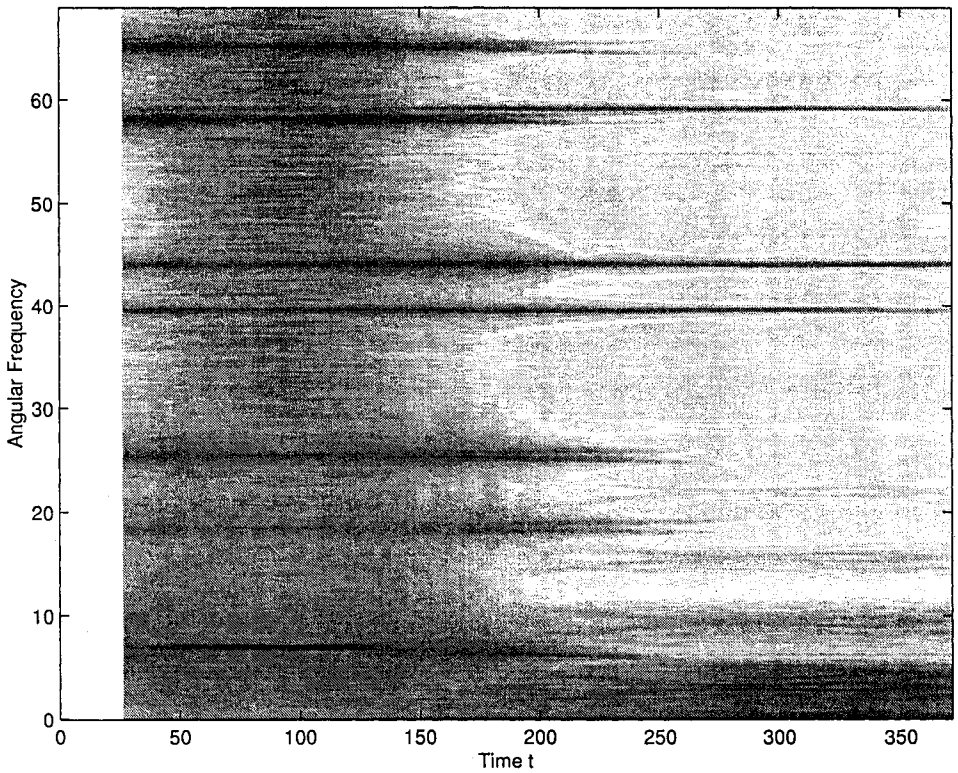

Figure 4.18: Spectrogram for the p mode of the mass, $m = 1$, $v_{t0} = 0.1$, $p_0 = 0.00001$, $q_0 = 0.00001$, $K_{dp} = 0.3$, $K_{dq} = 0.3$.

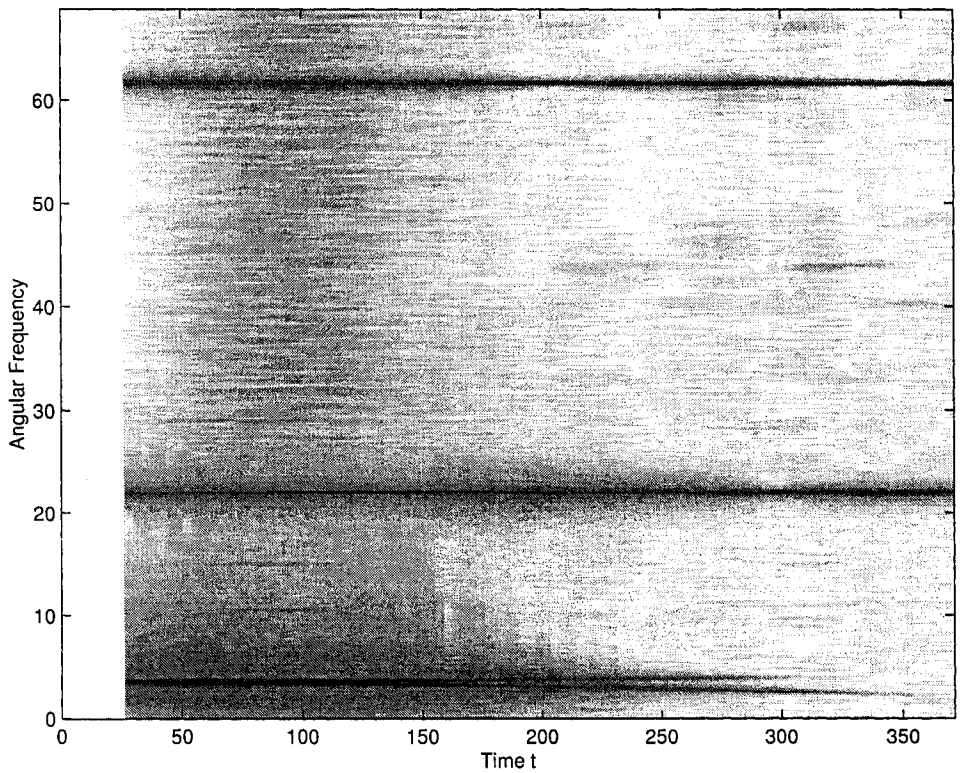

Figure 4.19: Spectrogram for the q mode of the mass. $m = 1$, $v_{t0} = 0.1$, $p_0 = 0.00001$, $q_0 = 0.00001$, $K_{dp} = 0.3$, $K_{dq} = 0.3$.

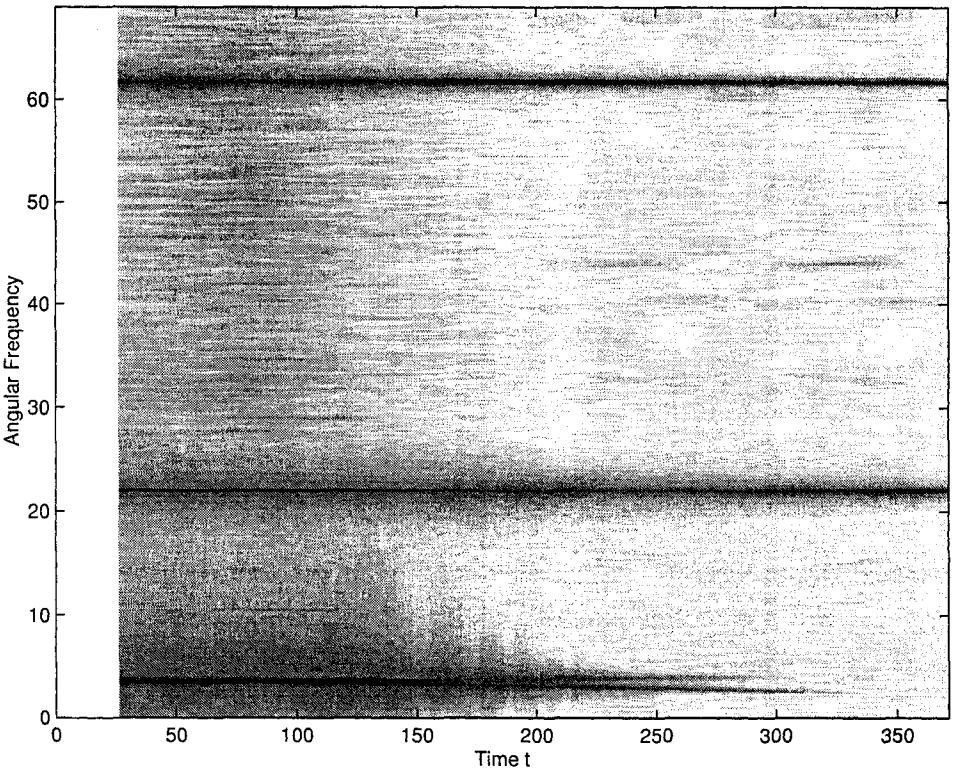

Figure 4.20: Spectrogram for the beam tip deflection v_{t0}. $m = 1$, $v_{t0} = 0.1$, $p_0 = 0.00001$, $q_0 = 0.00001$, $K_{dp} = 0.3$, $K_{dq} = 0.3$.

Next, we show simulation for the case where the initial value is given to the q mode of the moving mass using Parameter Set 4 in Table 4.1. The time response shown in Figure 4.21 indicates the rapid vibration suppression. These results can be compared to the undamped case shown in Figure 4.11. The power spectrum is shown in Figure 4.22. The time frequency spectrograms are shown in Figures 4.23-4.25. In this case, since the system is excited by a single mode (initial value is given to q only), energy is mostly exchanged between the lower harmonics. This is also indicated by the lack of higher frequency bands in the spectrograms.

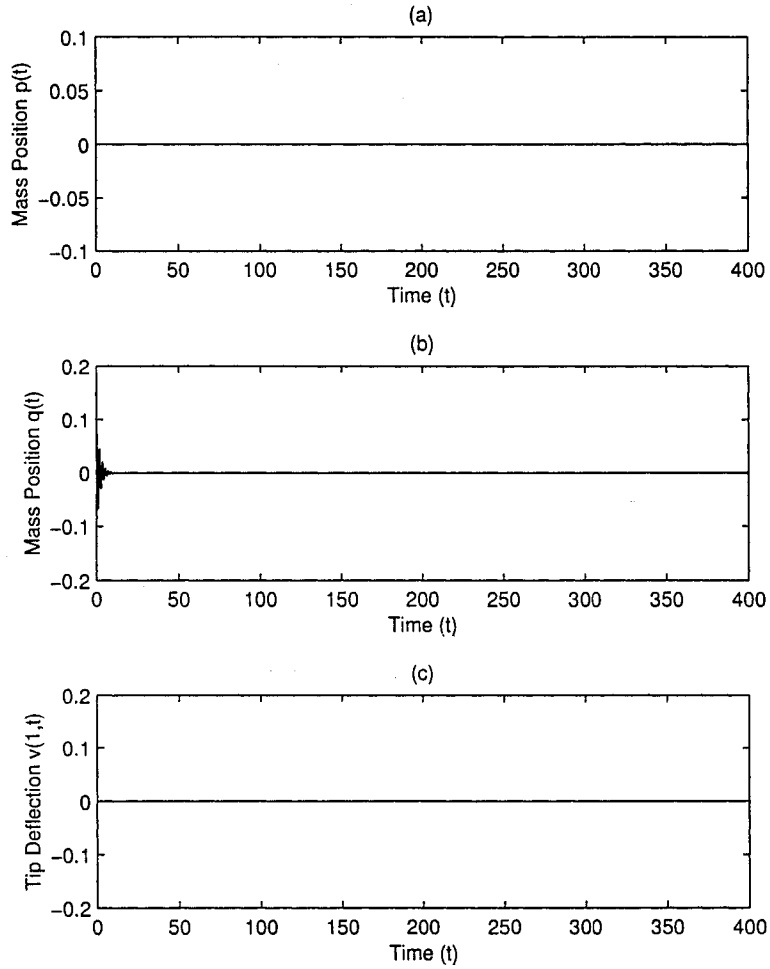

Figure 4.21: System response with damping, $m = 1$, $v_{t0} = 0.00001$, $p_0 = 0.00001$, $q_0 = 0.1$, $K_{dp} = 0.3$, $K_{dq} = 0.9$.(a) the p mode of the mass, (b) the q mode of the mass, (c) Beam tip deflection.

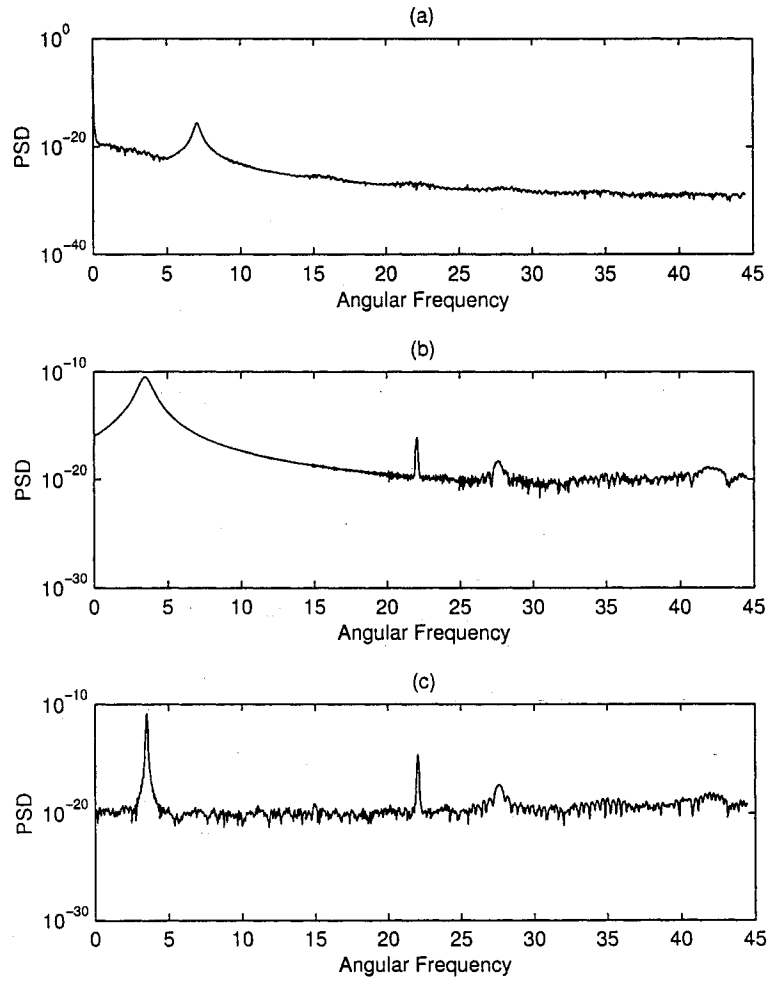

Figure 4.22: Power spectrum, $m = 1$, $v_{t0} = 0.00001$, $p_0 = 0.00001$, $q_0 = 0.1$, $K_{dp} = 0.3$, $K_{dq} = 0.9$.(a) the p mode of the mass, (b) the q mode of the mass, (c) Beam tip deflection

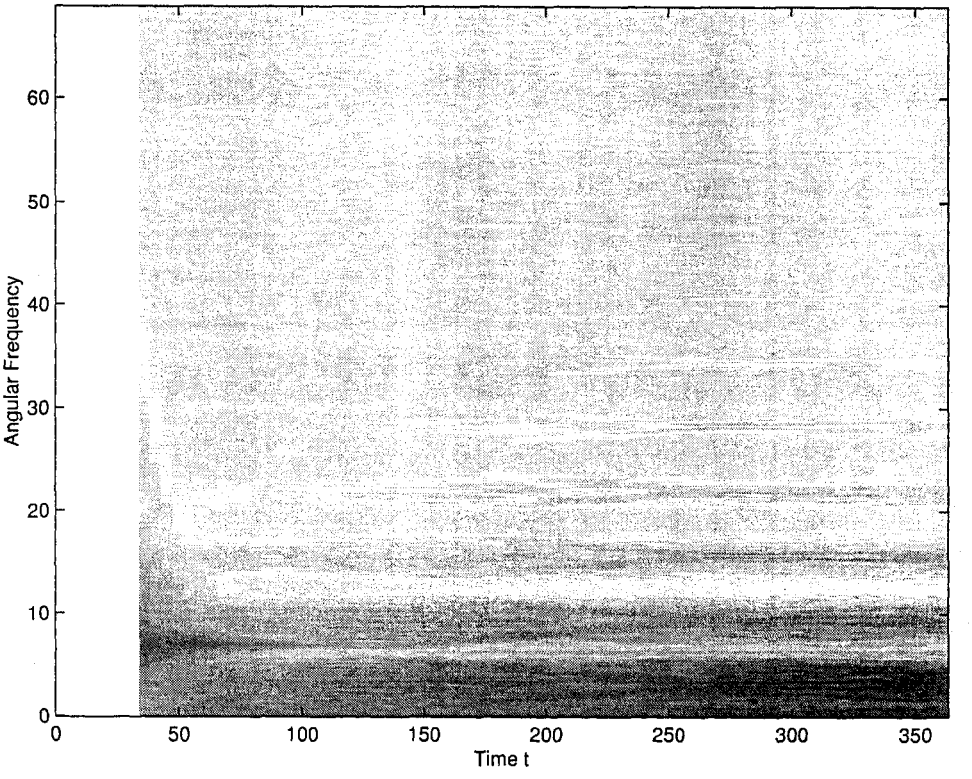

Figure 4.23: Spectrogram for the p mode of the mass, $m = 1$, $v_{t0} = 0.00001$, $p_0 = 0.00001$, $q_0 = 0.1$, $K_{dp} = 0.1$, $K_{dq} = 0.9$.

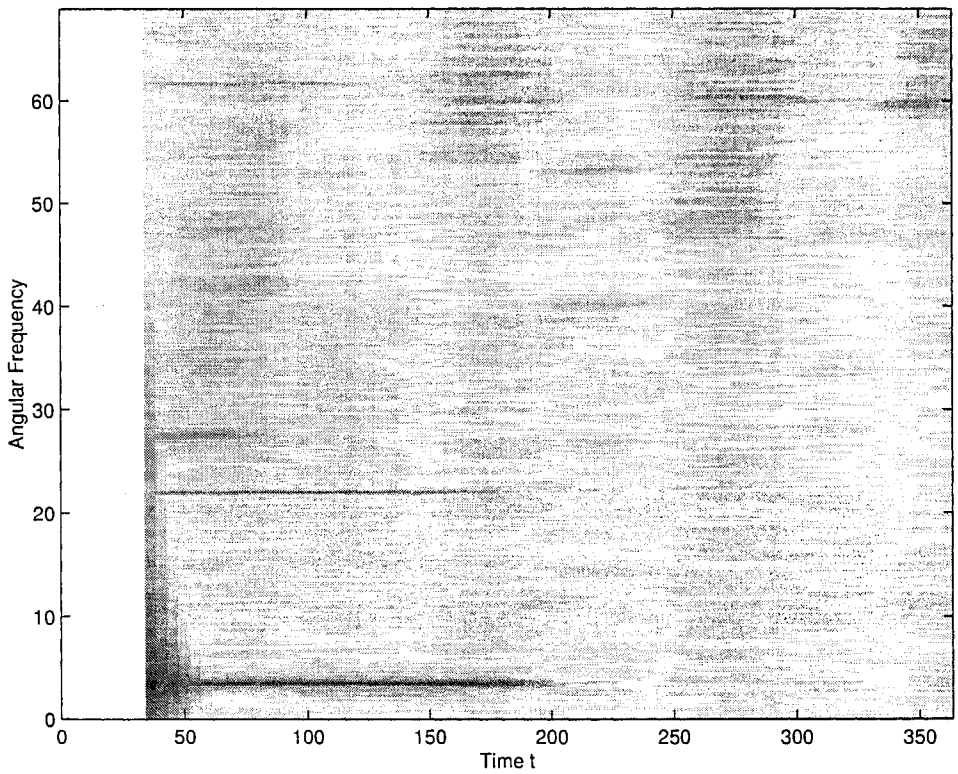

Figure 4.24: Spectrogram for the q mode of the mass, $m = 1$, $v_{t0} = 0.00001$, $p_0 = 0.00001$, $q_0 = 0.1$, $K_{dp} = 0.1$, $K_{dq} = 0.9$.

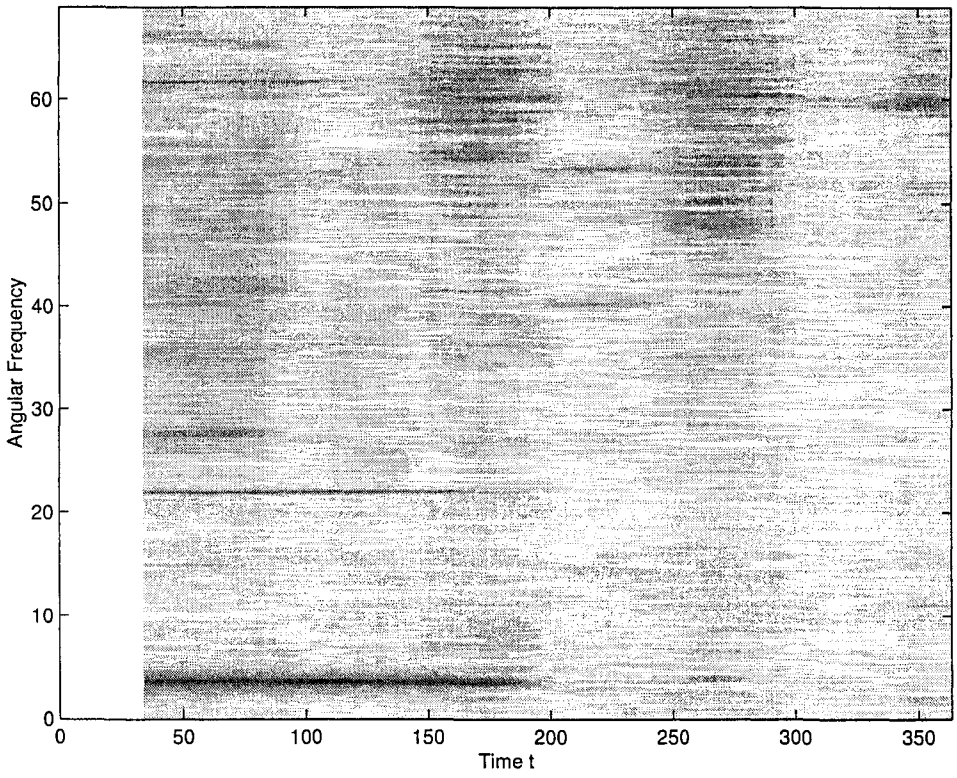

Figure 4.25: Spectrogram for beam tip deflection v_{t0}, $m = 1$, $v_{t0} = 0.00001$, $p_0 = 0.00001$, $q_0 = 0.1$, $K_{dp} = 0.1$, $K_{dq} = 0.9$.

In this chapter, the system response with and without internal resonance , with damping and without damping are simulated with setting initial value to the beam tip deflection and the q mode of the moving mass. Spectral characteristics are investigated using power spectrum graphs and time-frequency spectrograms. The results show that the vibration in the system can be suppressed successfully using the strategy presented in Chapter 3.

Chapter 5

Conclusion and Future Work

5.1 Conclusion

Contributions of this thesis can be divided into three parts: system modeling, parametric analysis and system response analysis. In system modeling, a cantilever beam carrying a traversing spring-mass subsystem was modeled. The coupling between the spring-mass subsystem and the beam is due to kinematic nonlinearities arising in the system as a result of the subsystem moving along the beam. The kinematic nonlinearities play a significant role in the system response. In particular, the system exhibits internal resonance under certain frequency conditions.

Another characteristic of the system is that as the traversing spring-mass subsystem moves along the length of the beam, the natural frequencies of the system change. In this thesis, this change in the natural frequencies was studied using parametric analysis.

The response of the system was analyzed through a numerical solution obtained

by reducing the nonlinear partial differential equations of motion to the ordinary differential equations using Galerkin method. The natural boundary conditions were incorporated into the equations of motion during this discretization process.

To suppress vibrations of the beam, internal resonance was established to strengthen the coupling between the spring-mass subsystem and the beam. Once strong coupling was established between the different vibration modes, vibration suppression was achieved by introducing damping using velocity feedback.

To obtain internal resonance, linear system natural frequencies were tuned to be commensuable by adjusting the stiffnesses of the spring-mass subsystem using position feedback.

For the system response analysis, equations of motion were solved using Adaptive Stepsize Runge-Kutta Method. System response without internal resonance and with internal resonance were compared. The effect of exciting the system by giving an initial value to the beam was compared with the case where the initial value was given to the q mode of the moving mass.

Vibration suppression strategy was demonstrated. It was shown that using the proposed vibration suppression strategy, the vibrations in the beam and in the spring-mass subsystem were quickly suppressed.

The time varying behavior of the system was studied using time-frequency spectrograms.

Perturbation method is a technique to obtain approximate analytical solution for nonlinear systems. Detailed description of the method can be found in [46]. Perturbation method was tried, but final result wasn't obtained due to the complexity

of the equations of motion of system. Partial results of the analysis are presented in Appendix A for future work.

5.2 Future Work

This thesis focused on vibration suppression for a cantilever beam carrying a traversing spring-mass subsystem. The system was assumed to undergo small amplitude vibration. The application of the vibration suppression strategy for the similar systems undergoing large amplitude vibration would be pursued. The experimental demonstration of the vibration suppression strategy would also be considered. Another objective of the future work is to establish the results using a semi-analytical method based on perturbation method.

Appendix A

Perturbation Method

The perturbation method of multiple scales is applied to solve the equations of motion of the system analytically. Although the final result isn't obtained yet, the procedure of solving the equations of motion using the perturbation method presented gives a broad view of solving nonlinear ODEs analytically.

A.1 Small Motions about the Equilibrium Position

In order to obtain a solution using the perturbation method of multiple scales, the equations of motion (2.30), (2.31) and (2.32) are further simplified by expanding them about the equilibrium positions $p = p_e$, $q = q_e$ and $\alpha_i = 0$. Using Taylor series expansion of (2.30), (2.31) and (2.32) about the equilibrium positions and

including terms up to the second derivative, the following equations are obtained:

$$\begin{aligned}
\ddot{p}+\ddot{s}+\omega_p^2 p+\dot{s}\left[\phi_i\phi_j''+\phi_i'\phi_j'\right]_{x=s(t)}\{\dot{\alpha}_i\alpha_j\} & \\
+\left[\phi_i\phi_j'\right]_{x=s(t)}\{\dot{\alpha}_i\dot{\alpha}_j+\ddot{\alpha}_i\alpha_j\} &= 0 \\
\ddot{q}+\omega_q^2 q+\left[\dot{s}\left[\phi_i'\right]_{x=s(t)}\{\dot{\alpha}_i\}+\left[\phi_i\right]_{x=s(t)}\{\ddot{\alpha}_i\}\right] &= 0 \\
m\left\{\left[\phi_i\phi_j\right]_{x=s(t)}\{\ddot{\alpha}_j\}+\ddot{q}\{\phi_i\}_{x=s(t)}\right. & \\
+\left[\phi_i\phi_j'\right]_{x=s(t)}\{(\ddot{p}+\ddot{s})\{\alpha_j\}+(2\dot{s}+\dot{p})\{\dot{\alpha}_j\}\} & \\
\left.+(\dot{s}\dot{p}+\dot{s}^2)\left[\phi_i\phi_j''\right]_{x=s(t)}\{\alpha_j\}\right\} & \\
+\left[\int_0^1\phi_i\phi_j dx\right]\{\ddot{\alpha}_j\}+\left[\int_0^1\phi_i''\phi_j'' dx\right]\{\alpha_j\} &= 0
\end{aligned} \tag{A.1}$$

In (A.1), for convenience, the same variables have been used to represent the motion about the equilibrium positions as in the original equations (2.30),(2.31) and (2.32).

A.2 Perturbation Analysis

In perturbation analysis, the first mode of a cantilever beam is used as the basis function in (A.1). Using only one basis function ϕ_1 and its corresponding coefficient function α_1. (A.1) is reduced to:

$$\begin{aligned}
\ddot{p}+\omega_p^2 p+d_1\ddot{\alpha}_1\alpha_1+d_1\dot{\alpha}_1^2+d_2\dot{\alpha}_1\alpha_1+d_3 &= 0 \\
\ddot{q}+\omega_q^2 q+d_4\ddot{\alpha}_1+d_5\dot{\alpha}_1 &= 0 \\
\ddot{\alpha}_1+\omega_1^2\alpha_1+d_6\ddot{q}+d_7\dot{\alpha}_1+d_8\ddot{p}\alpha_1+d_8\dot{p}\dot{\alpha}_1+d_9\dot{p}\alpha_1 &= 0
\end{aligned} \tag{A.2}$$

where $d_1, d_2, d_3, d_4, d_5, d_6, d_7, d_8, d_9$, and ω_1 are defined as:

$$
\begin{aligned}
d_1 &= \phi_1\phi_1' \Big|_{x=s(t)} & d_2 &= (\dot{s}\phi_1\phi_1'' + \dot{s}\phi_1\phi_1') \Big|_{x=s(t)} \\
d_3 &= \ddot{s} & d_4 &= \phi_1 \Big|_{x=s(t)} \\
d_5 &= \dot{s}\phi_1' \Big|_{x=s(t)} & d_6 &= \frac{m\phi_1}{\int_0^1 \phi_1^2 dx + m\phi_1^2} \Big|_{x=s(t)} \\
d_7 &= \frac{2m\dot{s}\phi_1\phi_1'}{\int_0^1 \phi_1^2 dx + m\phi_1^2} \Big|_{x=s(t)} & d_8 &= \frac{m\phi_1\phi_1'}{\int_0^1 \phi_1^2 dx + m\phi_1^2} \Big|_{x=s(t)} \\
d_9 &= \frac{m\phi_1\phi_1''\dot{s}}{\int_0^1 \phi_1^2 dx + m\phi_1^2} \Big|_{x=s(t)} & & \\
\omega_1^2 &= \frac{m\ddot{s}\phi_1\phi_1' + m\dot{s}^2\phi_1\phi_1'' + \int_0^1 \phi_1''^2 dx}{\int_0^1 \phi_1^2 dx + m\phi_1^2} \Big|_{x=s(t)} & &
\end{aligned}
\tag{A.3}
$$

where d_4-d_7 is the repeat of c_1-c_4 in (3.3) and redefined here for clarity. The reduced equation (A.2) is used to be analyzed with the method of multiple scales. The underlying idea of the method of multiple scales is to consider the expansion representing the response to be a function of multiple independent variables, or scales, instead of a single variable. In the current work, two time scales T_0 and T_1 are needed for the expansions, which are defined as below:

$$
\begin{aligned}
T_0 &= t \\
T_1 &= \epsilon t
\end{aligned}
\tag{A.4}
$$

ϵ is a scaling parameter. The linear motion of the system would be the primary motion on time scale T_0. The nonlinearities are expected to have a smaller effect and that effect will be on the slower time scale T_1. Using the chain rule, derivatives with respect to t become expansions in terms of the derivatives with respect to T_0

and T_1 as follows:

$$\begin{aligned} \frac{\partial}{\partial t} &= \frac{\partial}{\partial T_0} + \epsilon \frac{\partial}{\partial T_1} \\ \frac{\partial^2}{\partial t^2} &= \frac{\partial^2}{\partial {T_0}^2} + 2\epsilon \frac{\partial^2}{\partial T_0 \partial T_1} \end{aligned} \tag{A.5}$$

where the higher order term ϵ^2 is neglected in the second equation of (A.5).

The next step is to assume an asymptotic series solution for p, q and α_1. From (A.2), it can be seen that the highest nonlinearity of the equations need to be solved is quadratic nonlinearity. So two term asymptotic expansions for p, q and α_1 respectively are assumed as below:

$$\begin{aligned} p(t) &= \epsilon p_1(T_0, T_1) + \epsilon^2 p_2(T_0, T_1) \\ q(t) &= \epsilon q_1(T_0, T_1) + \epsilon^2 q_2(T_0, T_1) \\ \alpha_1(t) &= \epsilon u_1(T_0, T_1) + \epsilon^2 u_2(T_0, T_1) \end{aligned} \tag{A.6}$$

where $p_1(T_0, T_1)$, $q_1(T_0, T_1)$ and $u_1(T_0, T_1)$ are ϵ order solutions for p mode , q mode of the moving mass and defection of the beam. $p_2(T_0, T_1)$, $q_2(T_0, T_1)$ and $u_2(T_0, T_1)$ are ϵ^2 order solutions for p mode , q mode of the moving mass and defection of the beam. ϵ is a parameter introduced to obtain perturbation solution for nonlinear systems, which has no physical meaning and perturbation analysis doesn't supply the solution for ϵ. It is a parameter introduced as a device to track the nonlinearities and to allow the perturbation method to work in obtaining a solution. The closed form solution obtained using the perturbation method are the ϵ order terms p_1, q_1 and u_1.

Using (A.4) and (A.6), (A.2) is simplified and the ϵ and ϵ^2 terms are collected and setting them to zero gives:

ϵ order equations:

$$\begin{aligned}
\frac{\partial^2 p_1}{\partial {T_0}^2} + \omega_p^2 p_1 &= 0 \\
\frac{\partial^2 q_1}{\partial {T_0}^2} + \omega_q^2 q_1 + d_4 \frac{\partial^2 u_1}{\partial {T_0}^2} + d_5 \frac{\partial u_1}{\partial T_0} &= 0 \\
\frac{\partial^2 u_1}{\partial {T_0}^2} + d_7 \frac{\partial u_1}{\partial T_0} + \omega_1^2 u_1 + d_6 \frac{\partial^2 q_1}{\partial {T_0}^2} &= 0
\end{aligned} \tag{A.7}$$

ϵ^2 order equations:

$$\begin{aligned}
\frac{\partial^2 p_2}{\partial {T_0}^2} + \omega_p^2 p_2 &= -d_1 (\frac{\partial u_1}{\partial T_0})^2 - d_1 \frac{\partial^2 u_1}{\partial {T_0}^2} u_1 \\
&\quad -2 \frac{\partial^2 p_1}{\partial T_0 \partial T_1} - d_2 \frac{\partial u_1}{\partial T_0} u_1 \\
\frac{\partial^2 q_2}{\partial {T_0}^2} + \omega_q^2 q_2 + d_4 \frac{\partial^2 u_2}{\partial {T_0}^2} + d_5 \frac{\partial u_2}{\partial T_0} &= -2 \frac{\partial^2 q_1}{\partial T_0 \partial T_1} - 2 d_4 \frac{\partial^2 u_1}{\partial T_0 \partial T_1} - d_5 \frac{\partial u_1}{\partial T_1} \\
\frac{\partial^2 u_2}{\partial {T_0}^2} + d_7 \frac{\partial u_2}{\partial T_0} + \omega_1^2 u_2 + d_6 \frac{\partial^2 q_2}{\partial {T_0}^2} &= -d_9 \frac{\partial p_1}{\partial T_0} u_1 - d_8 \frac{\partial p_1}{\partial T_0} \frac{\partial u_1}{\partial T_0} - d_7 \frac{\partial u_1}{\partial T_1} \\
&\quad -2 d_6 \frac{\partial^2 q_1}{\partial T_0 \partial T_1} - d_8 \frac{\partial^2 p_1}{\partial {T_0}^2} u_1 \\
&\quad -2 \frac{\partial^2 u_1}{\partial T_0 \partial T_1}
\end{aligned} \tag{A.8}$$

The solution to (A.7) is:

$$\begin{aligned}
p_1 &= A_1(T_1) e^{i\Omega_1 T0} + \overline{A_1}(T1) e^{-i\Omega_1 T0} \\
q_1 &= A_2(T_1) e^{i\Omega_2 T0} + A_3(T_1) e^{i\Omega_3 T0} \\
&\quad + \overline{A_2}(T1) e^{-i\Omega_2 T0} + \overline{A_3}(T1) e^{-i\Omega_3 T0}
\end{aligned}$$

$$\begin{aligned} u_1 &= r_2 A_2(T_1)e^{i\Omega_2 T0} + r_3 A_3(T_1)e^{i\Omega_3 T0} \\ &\quad + \overline{r_2 A_2}(T1)e^{-i\Omega_2 T0} + \overline{r_3 A_3}(T1)e^{-i\Omega_3 T0} \end{aligned} \tag{A.9}$$

where Ω_n are the linear natural frequencies of the system and obtained as positive roots of the characteristic equation (3.6). Complex variables A_1,A_2 and A_3 are, in general, functions of the slower time scales. The over-bars in (A.9) represent the complex conjugate. Complex numbers r_n are eigen vectors corresponding to Ω_n and decided by :

$$r_n = \frac{-\omega_q^2 + \Omega_n^2}{\Omega_n(-d_4\Omega_n + id_5)} \tag{A.10}$$

Substituting p_1, q_1 and u_1 of (A.9) into the right hand side of (A.8), the following equations are obtained:

$$\begin{aligned} rhs4 &= -2i\frac{\partial A_1}{\partial T_1}\Omega_1 e^{i\Omega_1 T_0} \\ &\quad + (-id_2 + 2d_1\Omega_2)\Omega_2 r_2^2 A_2^2 e^{2i\Omega_2 T_0} + (-id_2 + 2d_1\Omega_3)\Omega_3 r_3^2 A_3^2 e^{2i\Omega_3 T_0} \\ &\quad + (d_1\Omega_2^2 + (-id_2 - 2d_1\Omega_3)\Omega_2 + d_1\Omega_3^2 + id_2\Omega_3)\overline{r_3 A_3} r_2 A_2 e^{iT_0(-\Omega_3+\Omega_2)} \\ &\quad + (d_1\Omega_2^2 + (2d_1\Omega_3 - id_2)\Omega_2 + d_1\Omega_3^2 - id_2\Omega_3) r_3 r_2 A_3 A_2 e^{iT_0(\Omega_3+\Omega_2)} + cc \\ rhs5 &= (-2i\Omega_2 - 2id_4 r_2\Omega_2 - d_5 r_2)\frac{\partial A_2}{\partial T_1}e^{i\Omega_2 T_0} \\ &\quad + (-d_5 r_3 - 2id_4 r_3\Omega_3 - 2i\Omega_3)\frac{\partial A_3}{\partial T_1}e^{i\Omega_3 T_0} + cc \\ rhs6 &= ((-d_7 - 2i\Omega_2)r_2 - 2id_6\Omega_2)\frac{\partial A_2}{\partial T_1}e^{i\Omega_2 T_0} \\ &\quad + ((-2i\Omega_3 - d_7)r_3 - 2id_6\Omega_3)\frac{\partial A_3}{\partial T_1}e^{i\Omega_3 T_0} \\ &\quad + (-id_9\Omega_1 + d_8\Omega_1^2 - d_8\Omega_1\Omega_2)\overline{r_2 A_2}_{A1} e^{iT_0(-\Omega_2+\Omega_1)} \\ &\quad + (-id_9\Omega_1 - d_8\Omega_1\Omega_3 + d_8\Omega_1^2)\overline{r_3 A_3} A_1 e^{iT_0(-\Omega_3+\Omega_1)} \end{aligned}$$

$$+(-id_9\Omega_1 + d_8\Omega_1\Omega_2 + d_8\Omega_1^2)r_2A_2A_1e^{iT_0(\Omega_1+\Omega_2)}$$
$$+(d_8\Omega_1\Omega_3 + d_8\Omega_1^2 - id_9\Omega_1)A_3r_3A_1e^{iT_0(\Omega_1+\Omega_3)} + cc \qquad \text{(A.11)}$$

where $rhs4$, $rhs5$ and $rhs6$ represent the right side of (A.8), cc are the conjugate terms. The homogeneous solution of (A.8) contains the terms $e^{i\Omega_1T_0}$, $e^{i\Omega_2T_0}$ and $e^{i\Omega_3T_0}$ which also appear in the right hand side of (A.8). This means, that the solution of (A.8) would contain secular terms that make the solution unstable. To eliminate the secular terms, the coefficients of $e^{i\Omega_1T_0}$, $e^{i\Omega_2T_0}$ and $e^{i\Omega_3T_0}$ in (A.11) are set to zero resulting in:

$$\begin{aligned} \frac{\partial A_1}{\partial T_1} &= 0 \\ \frac{\partial A_2}{\partial T_1} &= 0 \\ \frac{\partial A_3}{\partial T_1} &= 0 \end{aligned} \qquad \text{(A.12)}$$

From (A.12), it shows that A_1,A_2 and A_3 are constants and the ϵ order solution (A.9) is linear and depends only on the fast time scale T_0. Under this case, the coupling between the moving mass and the beam is very weak. So this solution is not pursued further. To get the solution for the system with strong coupling, the following relationship between the frequencies of the system Ω_1, Ω_2 and Ω_3 are presented:

$$\begin{aligned} \Omega_1 &= 2\Omega_3 + \epsilon\sigma_1 \\ \Omega_2 &= \Omega_3 + \epsilon\sigma_2 \end{aligned} \qquad \text{(A.13)}$$

where σ_n are small detuning parameters which quantitatively describes the nearness of Ω_1 to $2\Omega_3$ and Ω_2 to Ω_3. When σ_n are zero, we have a perfect $1:2:2$ ratio between Ω_n. This case is referred as $1:2:2$ IR. Under Internal Resonance conditions, the secular terms can't be eliminated by (A.12) any more because more terms contribute to the secular terms, which are shown as below:

$$\begin{aligned}
e^{2i\Omega_3 T_0} &= e^{i\Omega_1 T_0} e^{-i\sigma_1 T_1} \\
e^{2i\Omega_2 T_0} &= e^{i\Omega_1 T_0} e^{-i(\sigma_1 - 2\sigma_2) T_1} \\
&= e^{i\Omega_1 T_0} e^{-i\sigma_3 T_1} \\
e^{i(\Omega_2 + \Omega_3) T_0} &= e^{i\Omega_1 T_0} e^{-i(\sigma_1 - \sigma_2) T_1} \\
&= e^{i\Omega_1 T_0} e^{-i\sigma_4 T_1} \\
e^{i(\Omega_1 - \Omega_2) T_0} &= e^{i\Omega_3 T_0} e^{i(\sigma_1 - \sigma_2) T_1} \\
&= e^{i\Omega_3 T_0} e^{i\sigma_4 T_1} \\
e^{i(\Omega_1 - \Omega_3) T_0} &= e^{i\Omega_3 T_0} e^{i\sigma_1 T_1}
\end{aligned} \tag{A.14}$$

Using (A.14) in (A.11), it shows that the elimination of secular terms requires the following conditions:

$$\begin{aligned}
-2i\frac{\partial A_1}{\partial T_1}\Omega_1 + (2d_1 r_2^2 \Omega_2^2 - id_2 r_2^2 \Omega_2) A_2^2 e^{-i\sigma_3 T_1} \\
+(-id_2 r_3^2 \Omega_3 + 2d_1 r_3^2 \Omega_3^2) A_3^2 e^{-i\sigma_1 T_1} \\
+(d_1 r_2 \Omega_2^2 r_3 + (2d_1 r_2 r_3 \Omega_3 - id_2 r_3 r_2)\Omega_2 \\
+d_1 r_3 \Omega_3^2 r_2 - id_2 r_2 r_3 \Omega_3) A_3 A_2 e^{-i\sigma_4 T_1} &= 0
\end{aligned}$$

$$
\begin{aligned}
((-2i - 2id_4r_2)\Omega_2 - d_5r_2)e^{i\sigma_2 T_1}\frac{\partial A2}{\partial T_1} & \\
+((-2i - 2id_4r_3)\Omega_3 - d_5r_3)\frac{\partial A_3}{\partial T_1} &= 0 \\
((-2id_6 - 2ir_2)\Omega_2 - d_7r_2)e^{i\sigma_2 T_1}\frac{\partial A_2}{\partial T_1} & \\
+((-2id_6 - 2ir_3)\Omega_3 - d_7r_3)\frac{\partial A_3}{\partial T_1} & \\
+((d_8\Omega_1^2\overline{r}_2 + (-id_9\overline{r}_2 - d_8\overline{r}_2\Omega_2)\Omega_1)e^{i\sigma_4 T_1}\overline{A}_2 & \\
+(d_8\Omega_1^2\overline{r}_3 + (-d_8\overline{r}_3\Omega_3 - id_9\overline{r}_3)\Omega_1)e^{i\sigma_1 T_1}\overline{A}_3 A_1 &= 0 \qquad \text{(A.15)}
\end{aligned}
$$

The complex variables A_1,A_2 and A_3 can be converted to polar form using the relations:

$$
\begin{aligned}
A_1(T_1) &= \frac{1}{2}a_1(T_1)e^{i\varphi_1(T_1)} \\
A_2(T_1) &= \frac{1}{2}a_2(T_1)e^{i\varphi_2(T_1)} \\
A_3(T_1) &= \frac{1}{2}a_3(T_1)e^{i\varphi_3(T_1)} \qquad \text{(A.16)}
\end{aligned}
$$

where a_1, a_2 and a_3 are the modal amplitudes and φ_1, φ_2 and φ_3 are the corresponding phases. Substituting (A.16) in (A.15) gives equations for $\frac{\partial a_1}{\partial T_1}$, $\frac{\partial a_2}{\partial T_1}$, $\frac{\partial a_3}{\partial T_1}$, $\frac{\partial \varphi_1}{\partial T_1}$, $\frac{\partial \varphi_2}{\partial T_1}$ and $\frac{\partial \varphi_3}{\partial T_1}$. Those equations are too long and complicated to solve analytically at present. Perhaps semi-analytic approach should be pursued to solve the resulting equations. This is left as future work.

Bibliography

[1] I. H. Shames and C. L. Dym. *Energy and Finite Element Methods in Structural Mechanics.* Hemisphere Publishing Corporation, Taylor & Francis, Bristol, Pasadena, USA, 1985.

[2] A. Messac. Dynamics modelling of a flexible vehicle moving on the flexible rails of the flexible structure. AIAA-94-1614, pages 18–20, Hilton Heads,SC, April 1994. AIAA/ASME/ASCE/AHS/ASC 35th Structure,Structure Dynamics and Materials Conference.

[3] D.C.D. Oguamanam, J.S. Hansen, and G.R. Heppler. Dynamic response of an overhead crane system. *Journal of Sound and Vibration*, 213:889–906, 1998.

[4] G. G. Stokes. Discussion of a differential equation relating to the breaking of railway bridges. *Transactions of Cambridge Philosophical Society*, 8:707, 1849.

[5] S. Timoshenko. *Vibration Problems in Engineering.* Constable & Company, London, 1928.

[6] C. E. Inglis. *A Mathematical Treatise on Vibrations in Railway Bridges.* Cambridge University Press, London, 1934.

[7] L. Fryba. *Vibration of Solids and Structures under Moving Loads.* Noordhoff, Groningen, The Netherlands, 1972.

[8] M. M. Stanisic. On a new theory of the dynamical behavior of structures carrying moving masses. *Ingenieur-Archiv*, 55:176–185, 1985.

[9] S. Sadiku and H.H.E. Leipholz. On the dynamics of elastic systems with moving concentrated masses. *Ingenieur-Archiv*, 57:223–242, 1987.

[10] E.C. Ting, J. Genin, and J.H. Ginsberg. A general algorithm for moving mass problems. *Journal of Sound and Vibration*, 33:49–58, 1974.

[11] G. Michaltsos, D. Sophianopoulos, and A. N. Kounadis. The effect of a moving mass and other parameters on the dynamic response of a simply supported beam. *Journal of Sound and Vibration*, 191(3):357–362, 1996.

[12] D.M. Yoshida and W. Weaver. Finite element analysis of beams and plates with moving loads. *Publication of International Association for Bridge and Structural Engineering*, 31:179–195, 1971.

[13] T. Simkins. Transverse response of gun tubes to curvature-induced load functions. pages I67–I77, Waterliet,N.Y., 1978. Proceedings ,2nd US Army Symposium on Gun Dynamics,US Army Armament Research and Development Command.

[14] M. Olsson. Finite element, modal co-ordinate analysis of structures subjected to moving loads. *Journal of Sound and Vibration*, 99:1–12, 1985.

[15] M. Tanabe, Y. Yamada, and H. Wakui. Modal methods for interaction of train and bridge. *Computers and Structures*, 27:119–127, 1986.

[16] L. Vu-Quoc and M. Olsson. Computational procedure for interaction of high-speed vehicles on flexible structures without assuming known vehicle nominal motion. *Computer Methods in Applied Mechanics and Engineering*, 76:207–244, 1989.

[17] L. Vu-Quoc and M. Olsson. Formulation of a basic building block model for interaction of high speed vehicles on flexible structures. *Journal of Applied Mechanics,ASME*, 56:451–458, 1989.

[18] A. O. Cifuentes. Dynamic response of a beam excited by a moving mass. *Finite Elements in Analysis and Design*, 5:237–246, 1989.

[19] D.V. Hutton and J. Counts. Deflection of a beam carrying a moving mass. *Journal of Applied Mechanics, ASME*, 41:803–804, 1974.

[20] J. E. Akin and M. Mofid. Numerical solution for response of beams with moving mass. *Journal of Structural Engineering*, 115(1):120–131, January 1989.

[21] M. Olsson. On the fundamental moving load problem. *Journal of Sound and Vibration*, 145:299–307, 1991.

[22] M.A. Foda and Z. Abduljabbar. A dynamic green function formulation for the response of a beam structure to a moving mass. *Journal of Sound and Vibration*, 210:295–306, 1998.

[23] H.P. Lee. Dynamic response of a beam with a moving mass. *Journal of Sound and Vibration*, 191:289–294, 1996.

[24] H.P. Lee. Transverse vibration of a timoshenko beam acted upon by an accelerating mass. *Applied Acoustics*, 47:319–330, 1996.

[25] M.J. Balas. Direct velocity feedback control of space structures. *Journal of Guidance and Control*, 2(3):252–253, 1979.

[26] P.T. Kabamba and R.W. Longman. An integrated approach to optimal reduced order control. *The 3rd VPISU/AIAA Symposium on Dynamics and Control of Large Flexible Structures*, pages 571–585, 1981.

[27] M. Abdel-Rohman and H.H.E. Leipholz. Active control of flexible structures. *Journal of the Structural Division, ASCE*, 104(ST8):1251–1266, August 1978.

[28] J.-C Lo and B.T. Kulakowski. Active control of flexible beams subjected to external moving forces. *American Control Conference*, June 1993.

[29] M. Abdel-Rohman and H.H.E Leipholz. Automatic active control of structures. *Journal of the Structural Division, ASCE*, 106(ST3):663–677, March 1980.

[30] Frischgesell Thomas, Krzyzynski Tomasz, Bogacz Roman, and Popp Karl. On the dynamics and control of a guideway under a moving mass. *Heavy Vehicle Systems*, 6:176–189, 1999.

[31] Jiann-Chang Lo. Vibration control of a beam with moving mass. *Active control of Vibration and Noise,ASME*, 75:123–132, December 1994.

[32] S. Devasia, T. Meressi, B. Paden, and E. Bayo. Piezoelectric actuator design for vibration suppression:placement and sizing. *Journal of Guidance, Control and Dynamics*, 16:859–864, 1993.

[33] Y.-G. Sung. Modelling and control with piezoactuators for a simply supported beam under a moving mass. *Journal of Sound and Vibration*, 250:617–626, 2002.

[34] H.C. Kwon, M.C. Kim, and I.W. Lee. Vibration control of bridges under moving loads. *Computers and Structures*, 66(4):473–480, 1998.

[35] M. F. Golnaraghi. Vibration suppression of flexible structures using internal resonance. *Mechanics Research Communications Journal*, 18(2/3):135–143, 1991.

[36] M. F. Golnaraghi. Regulation of flexible structures via nonlinear coupling. *Journal of Dynamics and Control*, 1:405–428, 1991.

[37] K.L. Tuer, A.P. Duquette, and M.F. Golnarachi. Vibration control of a flexible beam using a rotational internal resonance controller, part 1: Theoretical development and analysis. *Journal of Sound and Vibration*, 167(1):41–62, 1993.

[38] A.P. Duquette, K.L. Tuer, and M.F. Golnarachi. Vibration control of a flexible beam using a rotational internal resonance controller, part 2: Experiment. *Journal of Sound and Vibration*, 167(1):63–75, 1993.

[39] S. A. Q. Siddiqui, M. F. Golnaraghi, and G. R. Heppler. Dynamics of a flexible

cantilever beam carrying a moving mass. *Nonlinear Dynamics*, 15:137–154, 1998.

[40] S. A. Q. Siddiqui, M. F. Golnaraghi, and G. R. Heppler. Dynamics of a flexible cantilever beam carrying a moving mass using perturbation, numerical and time-frequency analysis techniques. *Journal of Sound and Vibration*, 229(5):1023–1055, 2000.

[41] S. A. Q. Siddiqui, M. F. Golnaraghi, and G. R. Heppler. Internal resonance of a beam/traveling-mass system. Orlando, Florida, USA, November 5-10 2000. Proceedings of the Symposium on Control of Vibration and Noise-New Millennium, ASME International Mechanical Engineering Congress and Exposition.

[42] Singiresu S. Rao. *The Finite Element Method in Engineering.* Butterworth-Heinemann, third edition, 1998.

[43] E. Trefftz. *Handbüch der Physik.* Springer-Verlag, 1928.

[44] C. W. Gear. Ordinary differential equation techniques for partial differential equations. In K. Bathe, J. T. Oden, and W. Wunderlich, editors, *Formulations and Computational Algorithms in Finite Element Analysis*, chapter 24, pages 691–717. The Massachusetts Institute of Technology, 1977.

[45] W. H. Press, S. A. Teukolsky, W. T. Vetterling, and B.P. Flannery. *Numerical Recepies: The Art of Scientific Computing.* Cambridge University Press, Cambridge, second edition, 1992.

[46] A. H. Nayfeh and D. T. Mook. *Nonlinear Oscillations.* Wiley, New York, 1979.

[47] S. A. Q. Siddiqui and M. F. Golnaraghi. A new vibration regulation strategy and stability analysis for a flexible gyroscopic system. *Journal of Sound and Vibration*, 193(2):465–481, 1996.

[48] S. A. Q. Siddiqui and M. F. Golnaraghi. Vibration suppression in a flexible gyroscopic system using modal coupling strategies. *Journal of Mathematical Problems in Engineering*, 2:107–129, 1996.